Volume 19
Number 1
13 January 2026
Pages 1–400

Energy & Environmental Science

rsc.li/ees

ISSN 1754-5706

ROYAL SOCIETY OF CHEMISTRY

PAPER
Woojae Shin *et al.*
Toward a sustainable energy future using ammonia as an energy carrier: global supply chain cost and greenhouse gas emissions

Energy & Environmental Science

ROYAL SOCIETY OF CHEMISTRY

PAPER

View Article Online
View Journal | View Issue

Cite this: *Energy Environ. Sci.*, 2026, **19**, 162

Toward a sustainable energy future using ammonia as an energy carrier: global supply chain cost and greenhouse gas emissions

Woojae Shin, Haoxiang Lai, Gasim Ibrahim and Guiyan Zang *

A comprehensive techno-economic and environmental assessment database for global ammonia supply chains was developed across 63 countries, assessing diverse production technologies (gray, blue, yellow, pink, and green) and downstream logistics by quantifying the levelized cost of ammonia (LCOA) and life cycle greenhouse gas (GHG) emission using a harmonized framework. Results show significant global cost differentials; regions abundant in low-cost energy resources exhibit substantial economic advantages despite transport expenses, and imports can outperform domestic production in resource-constrained markets. GHG performance also varies; auto-thermal reforming ammonia with carbon capture demonstrates the lowest CO_2 avoidance costs, while green ammonia shows the lowest GHG intensity. Long-distance maritime transport can erode both cost and carbon advantages, underscoring the need to optimize trade corridors and logistics choices. Furthermore, a global decarbonization option analysis quantitatively confirmed that a full transition to blue ammonia could cut 70.9% GHG emission for a 23.2% total cost increase, while a full transition to green ammonia could achieve 99.7% GHG reduction for a 46.0% cost increase. This study provides the largest harmonized global ammonia supply chain dataset to date, providing a solid foundation for future research, enabling cross-country cost/emission comparisons and supporting supply-chain/investment optimization and policy design for deploying ammonia as a global energy carrier.

Received 21st September 2025,
Accepted 31st October 2025

DOI: 10.1039/d5ee05571g

rsc.li/ees

Broader context

Ammonia is emerging as a key enabler of a sustainable energy future. While traditionally vital for fertilizer production, its potential as a low-carbon energy carrier is poised to link major ammonia-producing and demand centers, reshaping global energy trade. Realizing this potential, however, requires a comprehensive understanding of the supply chain's economic and environmental implications. Currently, this holistic view is hindered by fragmented data/scope and inconsistent analytical methods. Our research addresses this knowledge gap by providing the first integrated techno-economic and greenhouse gas assessments of the global ammonia supply chain, encompassing various production technologies—including gray, blue, green, pink, and yellow ammonia—across 63 major countries. This analysis reveals significant cost and carbon differentials, identifying regional advantages and the impacts of long-distance transport. Critically, we quantify the low-carbonizing trade-offs: a full transition to blue ammonia could cut 70.9% of total GHG emissions for a 23.2% cost increase, while a green ammonia transition could achieve 99.7% GHG reduction for a 46.0% cost increase. This study provides the largest harmonized datasets and route-level maps for researchers, industry stakeholders, and policymakers to target infrastructure, standards and incentives at corridors that cut cost and emissions, accelerating a more secure and equitable global ammonia economy.

1. Introduction

Ammonia (NH_3) plays a critical role in the modern global economy as the foundation of nitrogen fertilizers that sustain agricultural productivity. About 70% of ammonia production is consumed in fertilizer manufacturing, bridging atmospheric nitrogen to the food supply.[1,2] The remainder serves various industrial uses (chemicals, explosives, and synthetic fibers).[1] This extensive use comes with a significant energy and carbon footprint: the Haber–Bosch process to synthesize ammonia from hydrogen (H_2) and nitrogen is energy-intensive and emits roughly 1.6 (natural gas steam methane reforming (SMR)) to 3.2 (coal gasification) tons of direct CO_2 per tonne NH_3 produced.[1] In 2020, ammonia production was responsible for about 450 million tonne CO_2, about 1.8% of global greenhouse gas (GHG) emissions.[3] These statistics underscore ammonia's current importance and the challenge of decarbonizing its supply

MIT Energy Initiative, Massachusetts Institute of Technology, 77 Massachusetts Avenue, Cambridge, MA 02139, USA. E-mail: guiyanza@mit.edu

chain. Beyond its fertilizer role, ammonia attracts interest as a potential carbon-free energy carrier and hydrogen storage medium. Containing 17.6% hydrogen by weight, ammonia can be liquefied under mild conditions (about 10 bar at ambient temperature or at −33 °C at 1 bar),[3] making it easier to store and transport than gaseous hydrogen. Also, global distribution infrastructure for NH_3 already exists – roughly 176 million tonnes are produced annually, and ~10% is traded internationally by tankers.[1] This positions ammonia as a promising and proven transporting vector for low-carbon energy: it can be synthesized using green or blue hydrogen and shipped from regions rich in solar and wind resources or ones with abundant natural gas resources with CO_2 sequestration capabilities to energy-importing markets. From a demand sector point of view, ammonia can be used directly as a zero-carbon fuel in thermal power plants, industrial furnaces, and maritime shipping, or it can be ''cracked'' back into hydrogen at the point of use for fuel cells and other hydrogen applications.[3] Early demonstrations have co-fired small fractions of ammonia in coal-fired boilers and gas turbines, demonstrating stable combustion.[4] Japan and Korea, for example, have included ammonia in their national hydrogen strategy and conducted trials blending ammonia in power generation.[5] These efforts indicate ammonia's potential to decarbonize sectors like shipping, power, rail, and heavy transport by direct combustion or by providing hydrogen on demand.[6,7] Table 1 shows that decarbonization-related ammonia applications such as power generation, hydrogen carriers, and ship fuels are projected to grow to nearly the same scale as traditional fertilizers and industrial uses by 2050 (43% of the total demand).[8] Because key sustainability and emission challenges (ammonia slip and reactive-nitrogen emissions) remain, ammonia is currently positioned as a longer-term (post-2040) pathway compared with options like methanol for shipping.[9] Furthermore, under the 1.5 °C scenario, which aims to limit the global average surface temperature to 1.5 °C above pre-industrial levels by the year 2100, these new applications are projected to expand even more, reaching 55% of the total demand. Additionally, the global ammonia supply chain map is characterized by net exporters/importers and self-sufficient countries, influenced by feedstock availability, supply–demand balance, pricing, geopolitics, and supply chain costs to target regions.[10] (Fig. 1 shows these historical trade patterns for global conventional ammonia.[11] The decadal difference highlights that these global trade flows are dynamic, responding to various factors including geopolitics and supply–demand shifts. This temporal variability is likely to intensify as low-carbon ammonia pathways emerge, introducing new cost structures and environmental-regulation constraints as key drivers of the global ammonia supply chain.) Considering these factors and anticipating a more diverse landscape of low-carbon ammonia production technologies with varying supply and demand countries in the future (particularly those having abundant renewable and low-carbon resources or targeting decarbonization with various carbon-reduction policies), the global ammonia supply chain requires development of indicators including low-carbon cost metrics and carbon intensity estimates.

Key technologies in the ammonia supply chain span several stages from production to end-use. The chain has four primary stages: (1) production: producing hydrogen and synthesizing ammonia *via* the Haber–Bosch process. This can be achieved through conventional or low-carbon pathways – *e.g.* 'gray ammonia' produced from fossil fuels (*via* natural gas steam methane reforming or coal gasification) without carbon capture, 'blue ammonia' from fossil fuels with carbon capture and storage (CCS), 'yellow ammonia' from water electrolysis using grid electricity, or 'green ammonia' using renewable electricity.[12] Although widely regarded as the most viable pathways for sustainable decarbonization,[7] these low-carbon routes often entail higher production costs and raise concerns regarding the large-scale availability of the energy-, water-, and land-resources required, compared to the conventional methods.[13–15] Emerging production methods (methane pyrolysis, electrochemical synthesis, *etc.*) are on the horizon but have not yet been broadly commercialized.[12,16] (2) Shipping & distribution: transporting ammonia from production sites to demand centers. Ammonia is shipped worldwide in refrigerated tankers (similar to LNG shipping, but close to room temperature and pressure). It can also be transported *via* pipelines, rail, or trucks in pressurized tanks. Geography and distance influence transport cost and emissions, and using ammonia-fueled ships can reduce tailpipe GHG emissions.[17] (3) Storage: storing ammonia in bulk at import/export terminals, production sites, and end-use locations. Ammonia's ease of liquefaction allows large-scale storage in refrigerated tanks at near-atmospheric pressure, or even in salt caverns, with both mass and volumetric energy density around 30–40% that of petroleum products. This makes ammonia a viable medium for seasonal energy storage and stockpiling hydrogen in a compact form. (4) Reconversion/utilization: converting ammonia to usable

Table 1 Historical and projected global ammonia demand [million tonnes per year] by sector (IRENA (2022)[8]). Despite cross-source variation, most outlooks foresee sharp post-2040 growth in new sectors (shipping fuel, hydrogen carrier, and power generation). See IRENA (2022)[8] for a multi-source comparison and DNV (2024)[9] for more recent estimates

	Stated policy scenario						1.5 °C scenario
Year	Fertilizer	Other existing uses	Shipping fuel	Hydrogen carrier	Power generation	Total	Total
2000	156	26	0	0	0	182	182
2010	166	29	0	0	0	195	195
2020	175	33	0	0	0	208	208
2030	185	36	1	1	3	226	303
2040	226	50	43	9	33	361	471
2050	267	65	77	110	63	582	740

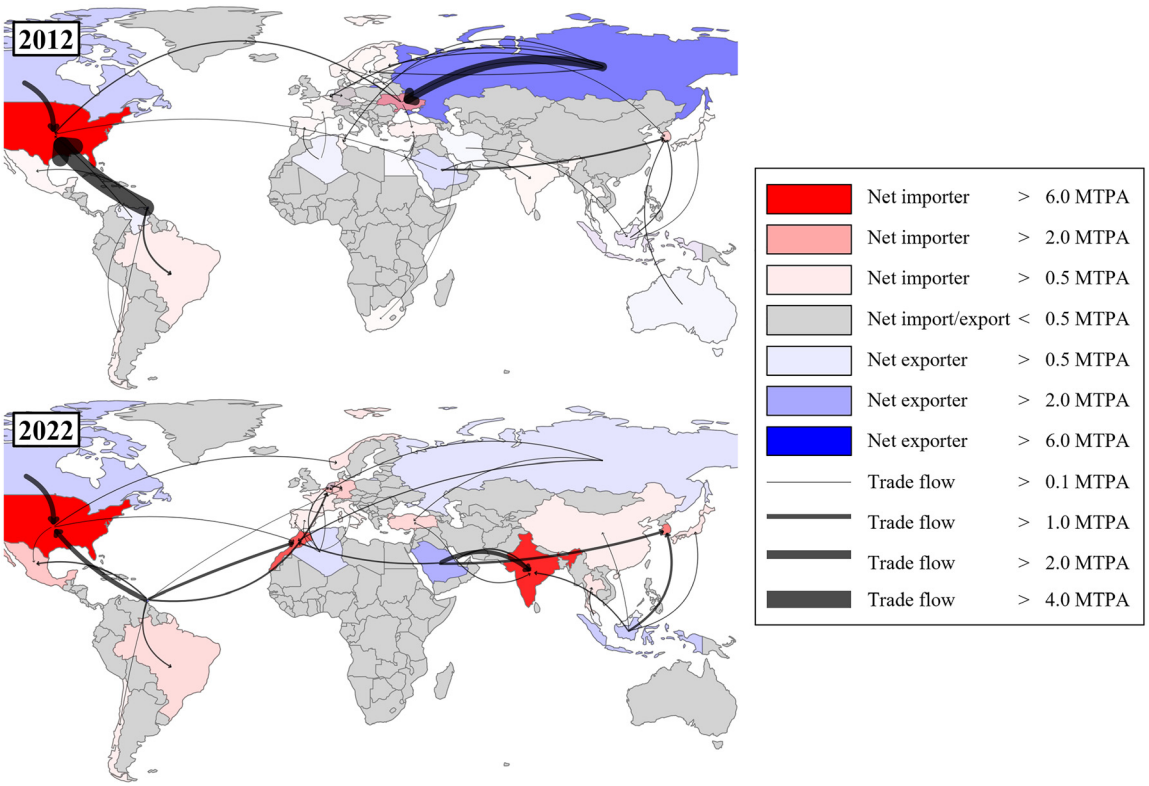

Fig. 1 Historical global ammonia trade flows and major player countries (CEPII BACI international trade database[11]).

energy or products at the destination. These stages include direct utilization (*e.g.*, burning ammonia in a power plant or ship engine or using it in fuel cells) and reconversion to hydrogen *via* catalytic ammonia cracking. Cracking technology is advancing, but it requires high temperatures (typically 500–600 °C) and leads to efficiency losses – about 13–15% of the energy content can be lost in reconversion.[7,18] This inefficiency has led most analyses to suggest avoiding ammonia cracking when possible, favoring direct ammonia use in applications.[19] In cases where pure hydrogen is needed (for fuel cells or industrial processes), improving cracker catalysts and heat integration is crucial.[20] Whereas the foregoing discussion has centered on large-scale plants which dominate global systems, recent work also examines decentralized, small-scale ammonia production co-located with demand, which could lessen reliance on long-haul logistics and reduce delivered costs and emissions.[21,22]

Despite ammonia's promise in the clean energy transition, significant gaps remain in comprehensive techno-economic analysis (TEA) and life cycle assessment (LCA) on GHG emissions. While numerous studies have examined ammonia production decarbonization or specific routes (focusing on specific technologies such as green or blue ammonia and specific supply chain corridors), there is a lack of comprehensive and harmonized analysis covering the entire supply chain, including current and prospective technologies. Table 2 synthesizes the scope and technological coverage of key previous studies and databases in this field, highlighting the fragmented nature of the research on ammonia supply chains. Table 2 shows significant research and database gaps in the current ammonia supply chain literature. First, there is no single TEA or life cycle GHG emission database that aggregates ammonia production together with global trade flows. While numerous studies have examined specific aspects of the ammonia supply chain, these remain fragmented by geography, analysis type (GHG emission estimates or TEA), and/or technological scope (gray, blue, green, and yellow).

Studies emphasizing life cycle GHG emissions results on the ammonia supply chain include Liu *et al.*,[26] Boyce, *et al.*,[37] Bicer and Dincer,[39] Dong *et al.*,[40] Huang *et al.*,[42] Sphera Solutions,[46] and Shin *et al.*[47] Liu *et al.*[26] conducted an environmental analysis limited to U.S. production, Boyce *et al.*[37] expanded to 26 countries, Sphera Solutions[46] provided global coverage but concentrated on maritime applications, and Shin *et al.*[47] focused on export of ammonia from major countries to Korea.

TEA studies that are focused on the economic performance of the ammonia supply chain are also included in Table 2. The IEAGHG study[23] conceptually addressed conventional and blue ammonia production pathways, and Alfa Laval *et al.*[24] additionally focused on green ammonia production. Morgan *et al.*,[27] Nayak-Luke *et al.*,[29] Rivarolo *et al.*,[33] and Kakavand *et al.*[36] performed region-specific analysis of green ammonia in the U.S, Scotland, Paraguay, and Iran, respectively. Nosherwani and Neto[30] compared gray ammonia and green ammonia costs in Germany. While some analyses consider broader regions,[31,32,38] they often exclude the downstream supply chain. Conversely, studies that consider multiple portions of the supply

Table 2 Comparison of previous ammonia supply chain analysis studies and this study. (P: production, T: transportation (pipeline, truck, *etc.*), Sh: shipping, B: bunkering, St: storage, R: reconversion, U: utilization); 'O' indicates that the category was included within the scope of the study and 'X' indicates that category was not within the scope of the study. 'GHG' denotes life cycle greenhouse gas emission analysis; full LCA, which conducts multi-environmental metrics, is even rarer in this field

		Scope					Production technology			
Authors	Year	Supply chain	Geography	Global	GHG	TEA	Gray	Blue	Green	Yellow
IEAGHG[23]	2017	P	Conceptual	X	X	O	O	O	X	X
Alfa Laval *et al.*[24]	2020	P	Conceptual	X	X	O	O	O	O	X
K. Lee *et al.*[25]	2022	P	United States	X	O	O	O	O	O	O
X. Liu *et al.*[26]	2020	P	United States	X	O	X	O	X	O	X
E. R. Morgan *et al.*[27]	2017	P	United States	X	X	O	X	X	O	X
P. Mayer *et al.*[28]	2023	P	Saudi Arabia	X	O	O	O	O	O	X
R. Nayak-Luke *et al.*[29]	2018	P	Scotland	X	X	O	X	X	O	X
S.A. Nosherwani and R. C. Neto[30]	2021	P	Germany	X	X	O	O	X	O	X
L. Pan *et al.*[31]	2023	P	China and the Middle East	X	X	O	O	X	O	X
C. A. Del Pozo and S. Cloete[32]	2022	P	Germany, Spain, Saudi Arabia	X	X	O	O	O	O	X
M. Rivarolo *et al.*[33]	2019	P	Paraguay	X	X	O	X	X	O	X
M. Tjahjono *et al.*[34]	2023	P	Indonesia	X	O	O	O	O	O	X
S. Vinardell *et al.*[35]	2023	P	Spain	X	O	O	O	X	O	X
S. Kakavand *et al.*[36]	2023	P	Iran	X	X	O	X	X	O	X
J. Boyce, *et al.*[37]	2024	P	Global (26 countries)	**O**	**O**	**X**	**O**	**O**	**O**	**O**
R. Nayak-Luke and R. Bañares Alcántara.[38]	2020	P	Global (70 countries)	O	X	O	X	X	O	X
Y. Bicer and I. Dincer[39]	2018	P, U	United States	X	O	X	X	X	O	X
IRENA[7]	2022	P, T, Sh, St, R	Conceptual	X	X	O	X	O	O	X
Clean Air Task Force[18]	2023	P, T, Sh, St, R	7 Countries → EU	X	X	O	X	O	X	X
D. T. Dong, *et al.*[40]	2024	P, T, U	Norway → Netherlands	X	O	X	X	O	O	X
C. F. Guerra *et al.*[41]	2020	P, St, Sh	Chile → Japan	X	X	O	X	X	O	X
J. Huang *et al.*[42]	2022	P, T, B, St, U	China and the Middle East	X	O	X	O	X	O	X
Hydrogen Europe[43]	2023	P, T, Sh, St, U	Europe	X	O	O	O	O	O	O
ISPT[44]	2016	P, T, Sh, St, U	Netherlands	X	X	O	O	O	O	O
T. Kroon, *et al.*[45]	2025	T, Sh, St	N. Africa → Europe (3 routes)	X	X	O	X	X	O	X
Sphera Solutions[46]	2024	P, Sh, St, B, U	Global	O	O	X	O	O	O	X
W. Shin *et al.*[47]	2023	P, T, Sh, St, R	Global → S. Korea	O	O	X	O	O	O	O
This study	**2025**	**P, T, Sh, St, R**	**Global ↔ Global (63 Countries)**	**O**	**O**	**O**	**O**	**O**	**O**	**O**

chain,[7,18,41,44,45] such as production to shipping or usage, often limit the analysis to smaller corridors and fewer countries.

Studies incorporating both GHG assessments and TEA include Lee *et al.*,[25] Mayer *et al.*,[28] Tjahjono *et al.*,[34] S. Vinardell *et al.*,[35] and Hydrogen Europe study.[43] Lee *et al.*[25] considered the gray, blue, green, and yellow ammonia, but focused only on the U.S. Mayer *et al.*[28] and Tjahjono *et al.*,[34] analyzed gray, blue, and green ammonia in Saudi Arabia and Indonesia, respectively. The Hydrogen Europe study[43] estimated various types of ammonia but focused on European countries only.

These categorizations highlight two critical gaps. First, to the best of the authors' knowledge, no existing study provides integrated TEA-life cycle GHG analysis with global trade coverage across the entire ammonia supply chain. Even studies with a global scope have methodological scope limitations. Second, comprehensive technology coverage (spanning gray, blue, green, and yellow ammonia) is rare, with only a few studies[25,43,44] addressing all production technologies, but each with geographical or analytical scope limitations. Compiling cost and GHG emission estimates from different studies across various countries and cases is methodologically inconsistent because each study applies different methodologies (*e.g.*, for GHG assessment: system boundary, impact assessment method, and inventory database; for TEA: country-specific economic parameters and calculation methods). Therefore, no reliable unified methodology exists for a comprehensive cost and GHG repository covering current and future ammonia supply chains. A unified methodology and research should: (i) apply key country-specific assumptions across geographies, (ii) track both cost and GHG intensity throughout the supply chain, and (iii) provide results for various current and future technologies.

In response to these gaps, this paper establishes a harmonized global TEA and life cycle GHG emissions analysis framework to systematically assess global ammonia production and trade. Through the integration of data and methodologies, this study facilitates consistent evaluation of ammonia's techno-economic viability and climate change impact across multiple production routes, transportation methods, and future decarbonization pathways. This structured approach addresses the lack of a harmonized global TEA and GHG emission database for ammonia production and trade. The manuscript is structured as follows: Section 2 presents the methodological framework and data sources for the TEA and GHG emission integration; Section 3 delineates the range of production, shipping and reconversion scenarios examined, integrated TEA and GHG performance across the inter-countries, sensitivity and renewable integration scenario impacts on the ammonia production pathways, and finally, the potential total supply chain cost and GHG reduction performance for existing and future feasible decarbonization pathway configurations.

2. Methodology and data

2.1. Scope

This study analyzes ammonia production and trade globally across 63 major countries, covering multiple conventional and low carbon production pathways and their associated supply chains. The analysis framework incorporates six ammonia production technologies: conventional gray ammonia production *via* steam methane reforming (SMR), blue ammonia production through SMR with CCS (SMR-CCS), auto-thermal reforming with air combustion and CCS (ATR-CCS-AC), or ATR with oxygen combustion and CCS (ATR-CCS-OC), and green ammonia production *via* both low-temperature electrolysis (LTE) and high-temperature electrolysis (HTE). Coal-based production pathways were excluded as they primarily serve domestic markets (especially in China[1]), whereas this study focuses on globally traded supply chains. The system boundary of this supply chain analysis spans upstream feedstock extraction and procurement through hydrogen and ammonia synthesis, pipeline transportation, port storage and loading, maritime shipping, port unloading and storage, and (where relevant) ammonia cracking back to hydrogen; end-use of ammonia or hydrogen is excluded. Captured CO_2 is assumed to be exported and to leave the system boundary as a liquefied CO_2 product.

Fig. 2 shows the global ammonia supply chain flow diagram as defined in this study's scope. As illustrated, ammonia for a specific country can be sourced through domestic or overseas imports. For domestically produced and consumed ammonia, direct utilization without reconversion to the hydrogen pathway is considered, thus avoiding reconversion efficiency losses. Imported ammonia can either be consumed directly or cracked for use in hydrogen form. Additionally, natural gas-based ammonia production pathways vary according to each country's natural gas procurement methods, resulting in either more complex procurement routes (LNG or PNG imports) or simpler routes (domestic NG production). For countries with limited natural gas resources that rely on LNG imports, the pathway of converting this "hard-won" imported LNG to ammonia for re-export is excluded from consideration due to economic implausibility. Furthermore, electrolysis-based ammonia pathways demonstrate significant variations in upstream processes depending on the electricity source (grid electricity mix, renewable energy, or nuclear power).

Following Subsections 2.2–2.4 describe in more detail about the methodology and data source. Mass and energy balances for ammonia production and downstream processes are detailed in Section 2.2. The ammonia production process is from modelling.[48] Other downstream processes' mass and energy balance and plant cost data are available in IEA (2019 and 2023) reports.[49,50] Also, TEA and life cycle GHG emission methodology are addressed in Sections 2.3 and 2.4, which are similar to the author's previous research, Hydrogen Carrier Analysis Tool (HyCAT).[51] More detailed methodology about prices and upstream life cycle GHG emissions (carbon intensity) of major feedstock and fuel (natural gas or electricity) has been referenced and calculated based on the separate literature and in-house models, as detailed more specifically in the supplementary information (SI).

2.2. Mass and energy balance

The mass and energy balance for ammonia production was developed using Aspen-plus models designed in the authors' previous research.[48] This previous study provided comprehensively designed mass-energy balance, plant scale, and economic data for SMR, SMR-CCS, ATR-CCS-AC, ATR-CCS-OC, LTE, and HTE technologies, all configured to achieve similar production capacities (approximately 0.8–1.1 million tonnes per year). Table 3 summarizes this mass and energy balance.

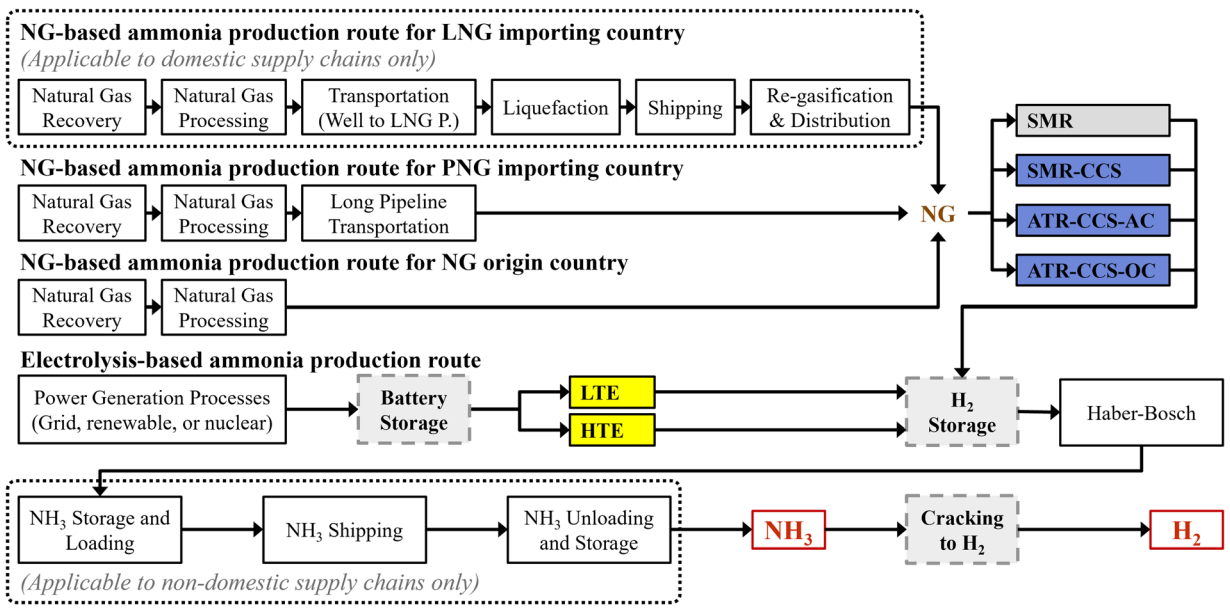

Fig. 2 Flow diagram of the global ammonia supply chain set in this study (processes in the dashed gray box is included only when specified).

Table 3 Mass and energy balance and major stream information on different NH_3 production plants[48]

	Unit	SMR	SMR-CCS	ATR-CCS-AC	ATR-CCS-OC	LTE	HTE
NG input	kg h^{-1}	70 979	75 472	60 000	60 000	0	0
Total electricity usage	GJ h^{-1}	329	429	288	211	5030	4110
NH_3 product flow	kg h^{-1}	109 974	109 969	103 294	91 484	128 640	113 840
Carbon capture ratio	%	—	96.20	95.60	99.40	—	—
Thermal efficiency	% (HHV)	61.10	56.40	68.70	62.10	57.40	62.20
CO_2 product–mass flow rate	kg h^{-1}	—	192 413	150 637	164 045	—	—
CO_2 product–pressure	bar	—	153	153	153	—	—
CO_2 product–temperature	Deg C	—	30	30	30	—	—
CO_2 product–CO_2 mole fraction	%	—	99.95	94.07	92.26	—	—
Onsite CO_2 emissions	$kgCO_2$ per $tonNH_3$	1711.64	69.69	67.83	10.64	—	—

As shown in Table 3, SMR-based pathways demonstrate higher HHV-based thermal efficiency compared to SMR-CCS, attributable to the thermal energy consumed by the reboiler for CCS (Selexol) operation and the consequent reduction in waste heat, resulting in lower self-generated power. Additionally, ATR-CCS-AC and ATR-CCS-OC exhibit a generally higher thermal efficiency than SMR-CCS because the oxygen requirements of ATR reformers enable advantageous process integration through utilization of residual oxygen produced in the ASU (while nitrogen serves as feedstock for the Haber–Bosch unit). Furthermore, ATR-CCS-OC achieves higher carbon capture rates than ATR-CCS-AC, resulting in substantially lower onsite CO_2 emissions compared to other blue ammonia processes. This superior performance stems from oxygen combustion generating syngas with higher CO_2 concentrations, which facilitates more efficient carbon capture. LTE represents the electrolysis pathway utilizing proton exchange membrane electrolysis cell (PEMEC) technology, while HTE employs solid oxide electrolysis cell (SOEC) technology which shows a slightly higher thermal efficiency than LTE.

The mass/energy balance for downstream processes is based on IEA (2019 and 2023) data.[49,50] For more information, please refer to the SI. All processes assume steady state and continuous input (*e.g.*, feedstock and fuel input profiles), resulting in high-capacity factor assumptions. For batch processes such as port storage and shipping, proper sizing and quantity determination for tanks or ships require consideration of amounts of ammonia delivered per year, reference storage tank or ship sizes, ship speed, and voyage distances. For this, the paper follows the heuristic optimization approach of the Hydrogen Carrier Analysis Tool (HyCAT).[51]

2.3. Techno-economic analysis

The TEA methodology follows the standardized framework established by the National Renewable Energy Laboratory's Annual Technology Baseline (NREL ATB).[52] This approach ensures consistency and comparability with the existing literature, which focused on other chemical or energy products such as hydrogen,[53] ethylene,[54] or electricity,[55] while providing robust economic evaluation across diverse geographical contexts. All monetary values expressed in this paper are on a 2022 USD basis. Note that the analysis excludes carbon policy- and certification-driven impacts on trade and costs (*e.g.*, carbon border adjustments, import duties, tax credits, and guarantees of origin[56]).

The levelized cost of ammonia (LCOA) or hydrogen (LCOH) is calculated using eqn (1)–(3) and expressed in 2022 USD per kg of ammonia (or hydrogen). The total cost required for delivering ammonia produced in an origin country 'o' to a target country 't' is defined as $LCOA_{tot,o\to t}$.

$$LCOA_{tot,o\to t} = \sum_{s\in S_A} L_{s,o\to t} \times LCOA_{s,j} \quad (1)$$

$$LCOH_{tot,o\to t} = LCOA_{tot,o\to t} \times \frac{H_{2,re}}{NH_{3,re}} + LCOH_{re,t} \quad (2)$$

The subscript 's' in eqn (1) refers to a stage in the supply chain, and 'j' denotes the country where that stage is located. S_A includes production, transportation 1 (pipeline between production and export harbor), loading and storage, shipping, unloading and storage, and transportation 2 (pipeline between the import harbor and the target ammonia usage site). The three stages preceding shipping are activities in the origin country ($j \equiv o$), while the subsequent two stages are activities in the target country ($j \equiv t$). $L_{s,o\to t}$ represents the accumulated ammonia loss factor from stage 's' to the Transportation 2 stage, derived from the stage-by-stage mass and energy balance. For shipping, the average value of economic parameters from both countries is applied.

$$LCOA_{s,j} = \frac{FCR_{s,j} \times CAPEX_{s,j} + FOM_{s,j}}{CF_s \times 8760(\mathrm{h\,year^{-1}})} + VOM_{s,j} + VOF_{s,j} \quad (3)$$

$CAPEX_{s,j}$, capital expenditure for stage 's' in country 'j', is calculated as the product of the total overnight cost (TOC) for stage 's', the location factor to adjust original CAPEX value for country j, and the ConFinFactor, which converts financing costs during the construction period into all-in capital cost. The TOC includes the total plant cost (TPC, see Table 4) and costs of process equipment, supporting facilities, direct and indirect labor, contractor services, and process and project contingency.[48] The fixed charge rate, $FCR_{s,j}$, is calculated using the weighted average cost of capital ($WACC_{s,j}$)—determined from country-specific debt and equity costs—and the ProFin-Factor, which accounts for the tax impact of depreciation methods (MACRS in this study). Fixed operation and maintenance costs ($FOM_{s,j}$) and variable operation and maintenance costs ($VOM_{s,j}$) for the production stage are based on modelling results as shown in Table 4, while subsequent downstream

Table 4 Economic analysis parameters for the NH_3 production plant (US based)[48]

	Unit	SMR	SMR-CCS	ATR-CCS-AC	ATR-CCS-OC	LTE	HTE
Capacity factor	%	90.0%	90.0%	90.0%	90.0%	97.0%	82.4%
TPC	Million $	635	940	803	871	1027	1116
TDCC	Million $	650	955	821	888	1476	1597
TNDCC	Million $	155	222	187	200	0	0
FOM	Million $	21	30	26	28	61	55
OVOM	Million $	11	18	15	15	0	0
WDC	Million $	0.016	0.069	0.069	0.069	0.000	0.000
IFC	Million $	15	15	18	17	0	0
Depreciation period	Years	20	20	20	20	20	20
Replacement period	Years	0	0	0	0	7	20

stages assume values of 4% and 0% of TOC, respectively. Variable operating fuel costs ($VOF_{s,j}$) represent costs from natural gas, electricity, marine diesel oil, and other fuels consumed in each stage. For more detailed equations and country-specific parameters calculated, please refer to the SI.

Fig. 3 illustrates key economic parameters that significantly influence country-wide comparative economic analyses: industrial grid electricity prices, natural gas prices, location factors, real WACC, and FCR (for detailed values, see SI.) Grid electricity and natural gas prices represent 20-year average values (considering inflation) where available, accounting for recent high volatility. These parameters are sourced from governmental energy statistic reports, tariff tables, and official global databases to ensure accuracy and reliability.

Renewable electricity LCOE represents the least expensive utility-scale renewable energy option (among solar photovoltaic, onshore wind, and hydropower) for each country, as reported by IRENA and IEA.[57,58] Location factors[59] were employed to adjust CAPEX for country-specific conditions, with the United States serving as the reference case (1.00). WACC is calculated based on country-specific inflation rates, risk-free rates, and risk and equity premiums[60] following IRENA's country-wide economic comparison study.[58] Regional average WACC values demonstrate geographical patterns: North America (7%), Europe (9%), Asia-Pacific (10%), Middle East (12%), South America (15%), and Africa (16%). These economic parameters exhibit substantial variation across countries, consequently resulting in significant inter-country FCR differentials. Notably, countries such as Egypt, Nigeria, Türkiye, Iran, and Argentina exhibit exceptionally high FCRs exceeding 45%.

2.4. Life cycle GHG assessment

This study estimates life cycle GHG emissions based on ISO 14040/14044 guidelines and the structure of the U.S. GREET 2022 model.[61] The life cycle scope includes Well-to-Gate (WTG), covering from feedstock extraction to ammonia production, and Well-to-Port (WTP), additionally covering the import process—scope most actively adopted by international initiatives related to clean ammonia and hydrogen.[62] Accordingly, this assessment scope includes all Scope 1 and Scope 2 emissions, as well as full upstream emissions (part of Scope 3). The analysis of life cycle GHG emissions excluding embodied emissions (indirect emissions from materials, equipment, and labor), aligning with major clean hydrogen regulations and guidelines.[63,64] For GHGs, global warming potentials (GWP) following IPCC 2021 AR6-100-year[65–67] horizon were adopted: 1 for CO_2, 29.8 for CH_4, and 273 for N_2O, with the functional unit expressed as kg CO_2 equivalent per kg of ammonia. For global analysis, country-specific upstream emissions (as shown in Fig. 4) were applied to calculate WTG emissions for each country or WTP emissions across all corridors.

The GHG emissions for ammonia are defined stage by stage in the following equations (eqn (4)–(6)). The WTG GHG emission ($GHG_{WTG,o,A}$) for ammonia originating from country 'o' is the sum of upstream lifecycle GHG emissions from feedstock (natural gas in this study), electricity used in the production process, and onsite CO_2 emissions. When this ammonia is transported to country 't', the WTP GHG emission of the delivered ammonia is the sum of WTG GHG emission (considering the accumulated loss factor) and the emissions from

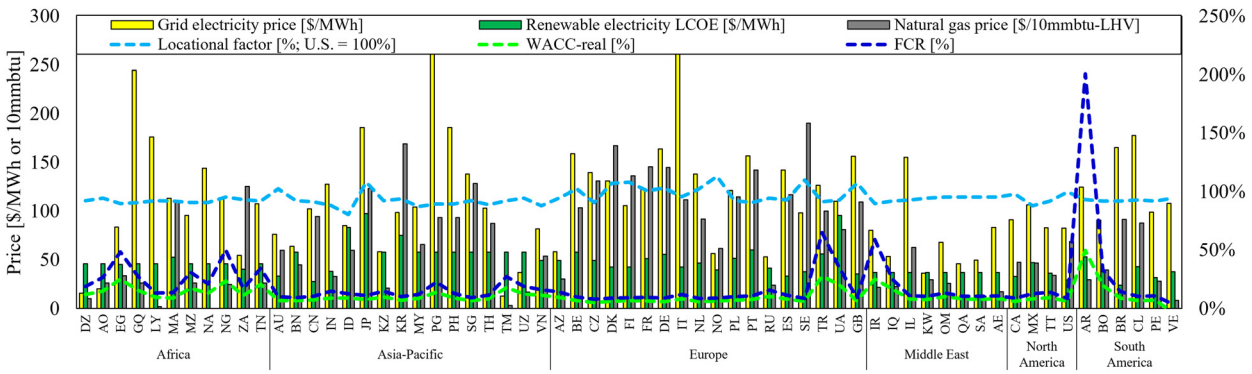

Fig. 3 Major TEA parameters (left axis: grid/renewable/NG price; right axis: location factor, WACC, and FCR). See detailed values in the SI.

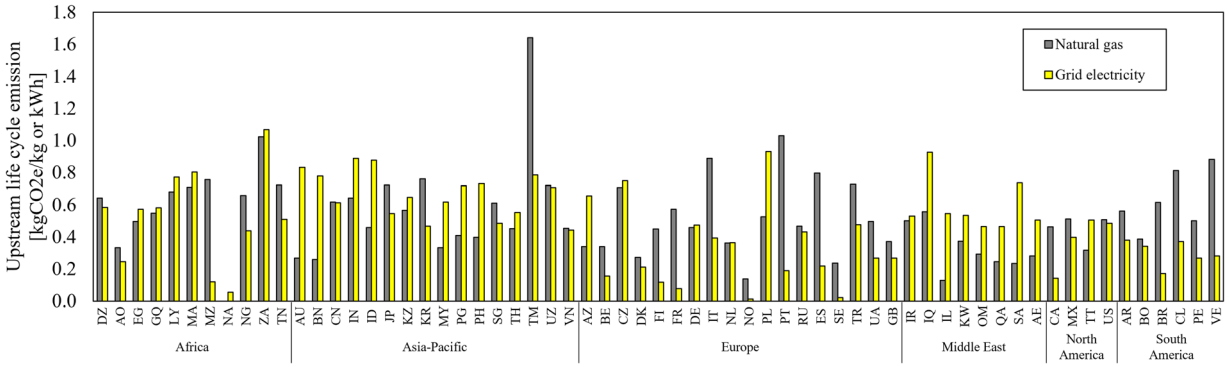

Fig. 4 Major life cycle GHG analysis parameters (upstream life cycle GHG emission of NG and grid electricity). See detailed values in the SI.

downstream processes ($GHG_{s,o\rightarrow t,A}$; onsite CO_2 emission + upstream life cycle emission of stage 's').

$$GHG_{WTG,o,A} = GHG_{p,o,NG} + GHG_{p,o,Elec} + GHG_{p,o,onsite\ CO_2} \quad (4)$$

$$GHG_{WTP,o\rightarrow t,A} = L_{p,o\rightarrow t} \times GHG_{WTG,o,A} + \sum_{s\in S_{d,A}} L_{s,o\rightarrow t} \times GHG_{s,o\rightarrow t,A} \quad (5)$$

$$\text{where, } S_{d,A} = \{s \in S_A | s \neq \text{production}\}$$

$$GHG_{WTP,o\rightarrow t,H} = GHG_{WTP,o\rightarrow t,A} \times \frac{H_{2,re}}{NH_{3,re}} + GHG_{re,o\rightarrow t,H} \quad (6)$$

To estimate the GHG emissions for each stage 's' ($GHG_{s,o\rightarrow t,A}$), the country-specific upstream life cycle GHG emissions of mix-averaged natural gas and grid electricity for the country where stage 's' occurs are required. In this study, the upstream life cycle GHG emission of the grid electricity mix was calculated by summing the 2021 upstream emissions, production emissions, and T&D loss emissions from IEA[68] and Carbon Footprint.[69] Additionally, a novel contribution of this study is the development of a comprehensive natural gas upstream life cycle emission calculator for 63 countries. This in-house model integrates multiple region-specific factors affecting upstream emissions of natural gas:

– Methane leakage (fugitive and vented) rates across recovery and processing stages

– Process efficiencies of NG recovery and processing

– Flaring emissions at associated or non-associated gas fields and liquefaction facilities

– Share of NG mix (domestic production, LNG import and PNG import ratios)

– Voyage and pipeline importing distances

For detailed calculation methods and background data regarding the upstream life cycle GHG emissions of country-specific natural gas and grid electricity, please refer to the SI.

3. Results

The comparative cost and life cycle GHG emissions were conducted for the global ammonia supply chain, spanning production technologies, shipping options, reconversion fuel options, and inter-country trade flows. The study was performed within the context of 63 major ammonia trading and production countries, with sensitivity analysis to identify key parameters affecting cost and emissions across the entire chain.

3.1. Performances of different technologies

3.1.1. Production. Fig. 5 illustrates the LCOA and life cycle GHG emissions for the six ammonia production technologies, using a 100 tonnes NH_3 per h production in the context of United States as a representative case. The SMR without CCS demonstrates the lowest production cost at \$0.48 per $kgNH_3$; however, this economic advantage is counterbalanced by the highest GHG emissions at 2.46 $kgCO_2e$ per $kgNH_3$. This significant emission profile is primarily attributed to onsite CO_2 emissions (approximately 70% of total emissions), with the remainder originating from upstream associated with natural gas and grid power generation. In contrast, SMR-CCS achieves an approximately 61% reduction in GHG emissions compared to conventional SMR, while incurring a 29% increase in production costs. This cost premium is attributable to additional capital expenditure for CO_2 capture equipment, associated fixed operating costs, and elevated electricity consumption for the capturing processes. The CO_2e avoidance cost for SMR-CCS relative to the conventional SMR is calculated at approximately \$85.1 per tonneCO_2e. In addition, the ATR-CCS-AC exhibits 10% higher costs than conventional SMR at \$0.51 per $kgNH_3$, while generating emissions of 0.75 $kgCO_2e$ per $kgNH_3$. This configuration yields a CO_2e avoidance cost of approximately \$20.1 per tonneCO_2e compared to the conventional SMR, representing a more cost-effective decarbonization pathway than SMR-CCS. ATR-CCS-OC demonstrates the lowest emissions among blue ammonia pathways at 0.66 $kgCO_2e$ per $kgNH_3$, with a production cost of approximately \$0.57 per $kgNH_3$, resulting in a CO_2e avoidance cost of \$48.8 per tonne-CO_2e. The superior performance of ATR-based blue ammonia compared to the SMR-based blue ammonia in both cost and emissions metrics is attributed primarily to enhanced process integration and CO_2 capture efficiency. This integration efficiently utilizes the primary outputs of the air separation unit (ASU)—oxygen for ATR combustion and nitrogen for the

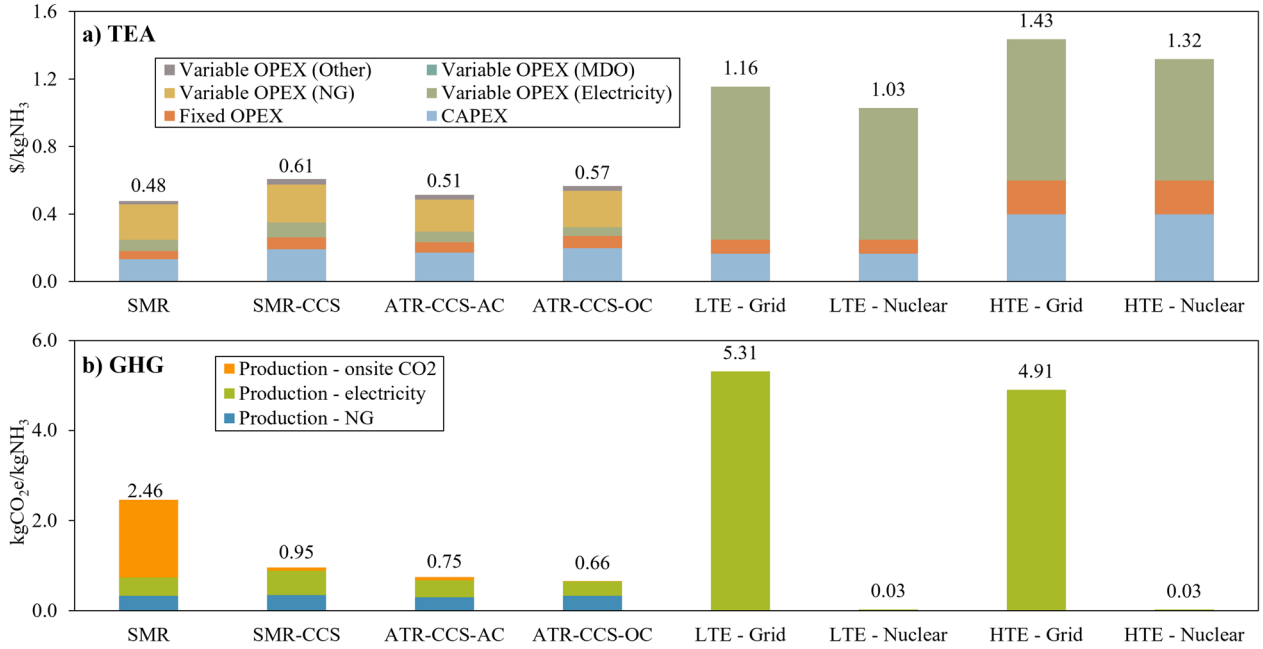

Fig. 5 (a) LCOA and (b) life cycle GHG emission of different NH_3 production technologies (US production, 100 tonnes NH_3 per h production).

Haber–Bosch process—without significant losses, achieving greater process synergies. Additionally, the higher CO_2 concentration in ATR syngas enables more efficient carbon capture, resulting in lower capital expenditure and reduced electricity consumption.

Also, Fig. 5 presents results for electrolytic ammonia *via* LTE and HTE, differentiated by electricity source (grid-powered yellow ammonia and nuclear-powered pink ammonia). The grid electricity scenario assumes that ammonia production plants purchase industrial electricity from the grid network, while the nuclear electricity scenario presupposes ammonia plant location in proximity to nuclear power facilities, enabling direct connection without transmission through extensive grid infrastructure or long-distance power lines. Both power sources provide consistent electricity supply profiles unlike variable renewable energy (VRE) sources, thus avoiding intermittent reduction in ammonia production capacity factors. For cost analysis of green ammonia utilizing dedicated renewable electricity, refer to Sections 3.2, 3.5, and 3.6. Electrolytic ammonia production generally demonstrates higher production costs compared to blue ammonia pathways. Under conditions of \$82 per MWh grid electricity prices[70] and \$71 per MWh nuclear power LCOE,[57] grid-powered electrolysis routes exhibited higher production costs than nuclear-powered routes in the context of the United States. HTE shows a larger capital expenditure impact on total LCOA at approximately 28%, compared to 14% for LTE. This differential is attributable to the process characteristics of HTE, having higher electrolyzer stack costs. From an GHG emission perspective, nuclear-powered electrolysis approaches near-zero emissions at 0.03 $kgCO_2e$ per $kgNH_3$ with a U.S. nuclear electricity carbon intensity of 3 $kgCO_2e$ per MWh.[61] In contrast, grid-powered electrolysis in the United States, with its not decarbonized electricity grid (485 $kgCO_2e$ per MWh), generates GHG emissions about 5 $kgCO_2e$ per $kgNH_3$, which is approximately double that of conventional SMR-based gray ammonia. This value underscores that electrolytic ammonia production utilizing insufficiently decarbonized grid electricity (above 250 $kgCO_2e$ per MWh) may prove disadvantageous compared to conventional gray ammonia production in both environmental and economic dimensions. Further analysis of the inter-country variations of these technologies is presented in Sections 3.2–3.5.

3.1.2. Shipping fuel. The economic and environmental performance of utilizing different shipping fuels for ammonia cargo transport vary according to the upstream cost and GHG emission differences between ammonia and conventional marine fuels on an energy-equivalent basis. Fig. 6 illustrates these impacts using the example of ATR-CCS-OC based blue ammonia from the United States and shipped to Japan case, comparing three shipping fuel scenarios: 100% marine diesel oil (MDO) utilization, a combination of MDO and NH_3 boil-off gas, and 100% NH_3 cargo as shipping fuel. This result excludes reconversion processes to account for direct ammonia usage cases such as coal-ammonia co-firing power generation. The MDO and MDO + NH_3 boil-off scenarios demonstrate nearly equivalent cost outcomes, attributable to the fact that NH_3 boil-off is consumed regardless of whether vented or utilized as fuel, and the energy substitution of MDO fuel by boil-off NH_3 is only 8.4% on the LHV basis. However, the shipping emission in the MDO + NH_3 boil-off case is lower by 0.01 $kgCO_2e$ per $kgNH_3$, confirming that shipping emission reduction is proportional to the MDO fuel substitution rate. Note that this study assumes zero GHG emissions from ammonia combustion, consistent with current carbon accounting methodologies employed in clean ammonia initiatives.[63,64] In contrast, utilizing 100% NH_3 cargo as shipping fuel results in higher cost and emissions in upstream processes; this option necessitates additional upstream processes such as production to

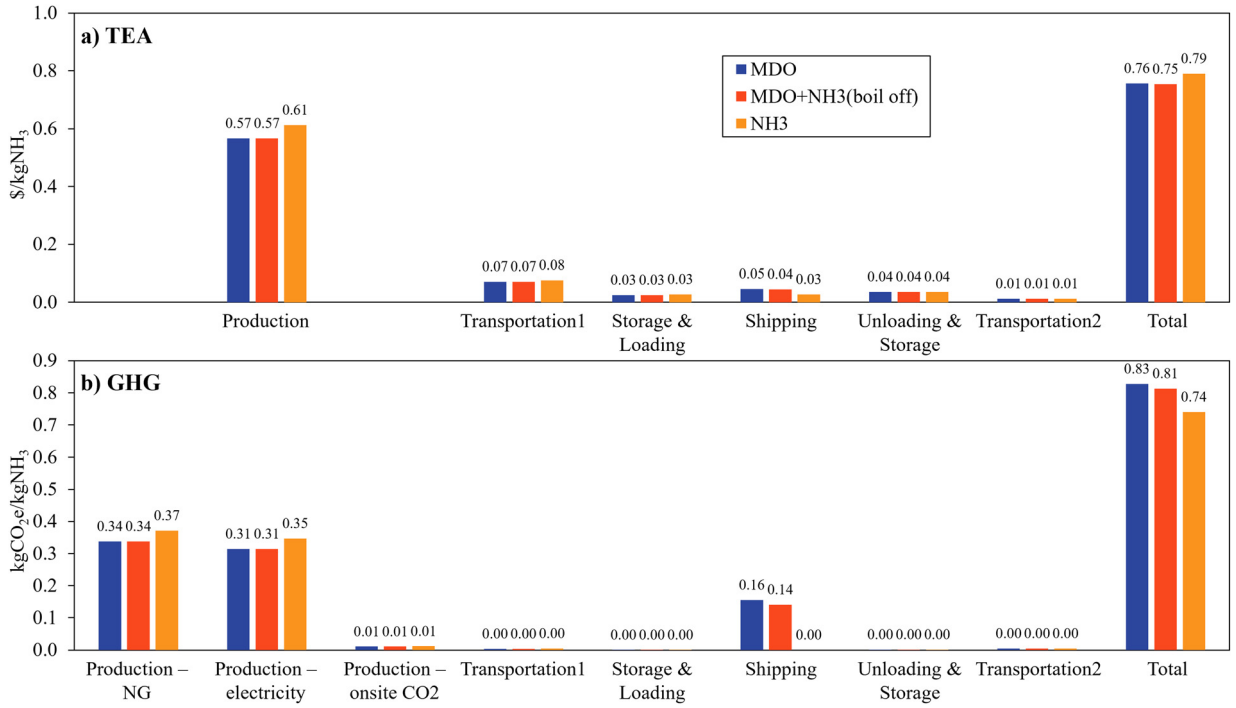

Fig. 6 Effects of shipping fuel option on (a) LCOA and (b) GHG emission (U.S. to Japan, ATR-CCS-OC, grid electricity use, no reconversion to H_2, 100 tonnes NH_3 per h delivery).

deliver an equivalent amount of ammonia cargo (amplification effect). In the U.S.-Japan scenario, where upstream ammonia production costs are beyond a certain range and emissions are relatively low, the 100% NH_3 cargo option exhibits the highest overall levelized cost of ammonia (LCOA) while simultaneously achieving the lowest emission performance. The optimal shipping fuel strategy from economic or environmental perspectives depends on whether ammonia production costs exceed those of conventional fuels (on an energy-equivalent basis) and whether upstream emissions exceed the carbon intensity of traditional fuels (including both upstream emissions and combustion emissions). Similarly, blue and green ammonia (as opposed to gray) render ammonia cargo utilization as shipping fuel emissions advantageous.

3.1.3. Reconversion fuels. The comparison of economic and environmental performance of utilizing different reconversion fuels (ammonia, natural gas, or electricity) for hydrogen reconversion from transported ammonia, analogous to shipping fuel comparisons, relies on the cumulative upstream costs and emissions of these candidate fuels on an energy-equivalent basis. Fig. 7 illustrates these impacts using the example of ATR-CCS-OC blue ammonia from the United States and shipped to the Japan case, comparing three reconversion fuel scenarios: ammonia self-consumption, natural gas combustion, and grid electricity utilization *via* electric crackers. When ammonia serves as reconversion fuel, approximately 20% of the input ammonia is combusted for the endothermic cracking reaction, necessitating amplification of upstream process costs. In the U.S.-to-Japan transportation scenario, the cumulative upstream cost of ammonia remains higher relative to natural gas on the LHV-basis, resulting in an overall LCOH approximately 10% higher than the natural gas option. The grid electricity pathway demonstrates the highest cost, attributable to the highest energy price per energy unit (MJ) of electricity compared to natural gas or ammonia—a condition that persists across most geographical regions. While scenarios with electricity prices below natural gas prices in equal energy content basis could theoretically render the electricity pathway most cost-effective, such circumstances remain rare. From a GHG emission perspective, the ammonia fuel pathway similarly exhibits amplification of upstream process emissions. However, the reconversion process itself generates minimal emissions when utilizing ammonia (showing the minor contribution from auxiliary electricity consumption), as ammonia combustion produces zero GHG emissions. This favorable emission profile in the reconversion stage outweighs the upstream amplification effect in most corridor cases, resulting in the lowest overall life cycle GHG emissions. In the case of regions characterized by exceptionally low upstream emissions from natural gas and grid electricity—particularly countries like Norway with notably clean natural gas production and substantially decarbonized electricity grids—the ammonia-fueled reconversion may exhibit the lowest emission profile showing a larger gap. Consequently, the optimal reconversion fuel selection from both economic and GHG emission perspectives depends fundamentally on the relative positioning of ammonia's upstream costs and emissions compared to competing fuels in the target regional context.

3.2. Domestic production in different countries

This section presents the TEA and life cycle GHG results for blue ammonia and electrolytic ammonia production across

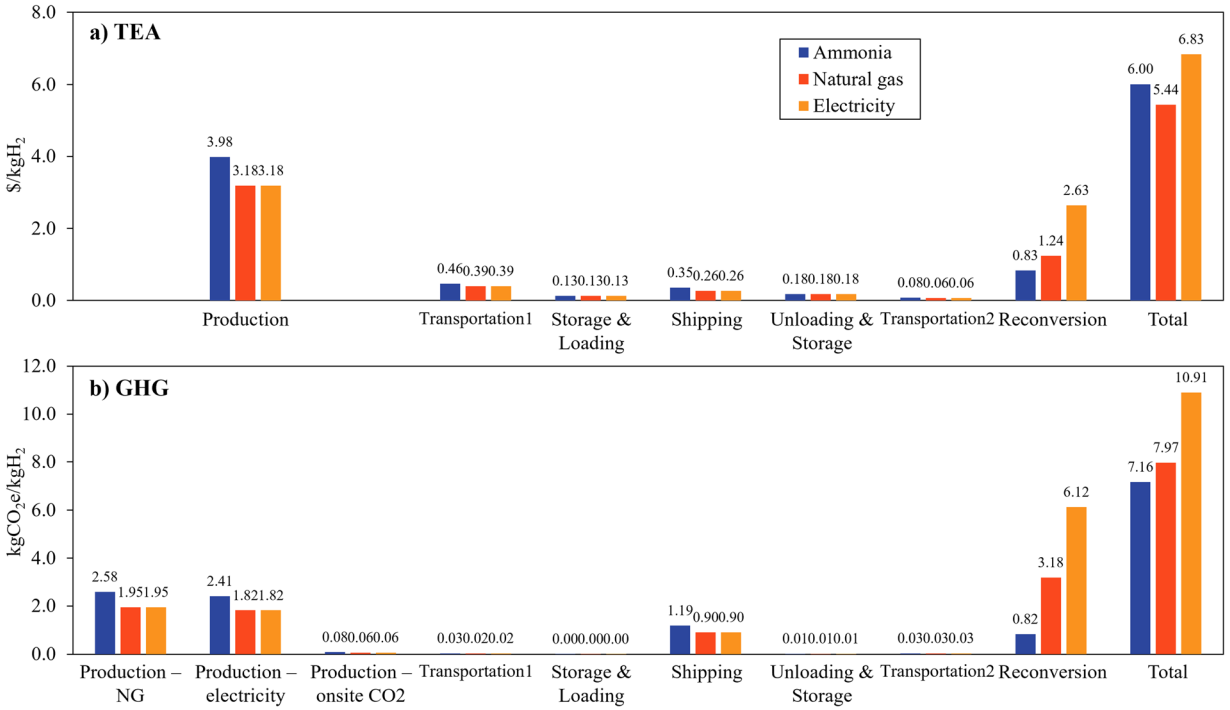

Fig. 7 Effects of reconversion fuel option on (a) LCOH and (b) GHG emission (U.S. to Japan, ATR-CCS-OC, grid electricity use, MDO for shipping fuel, 17.2 tonnes H_2 per h delivery).

different countries. Fig. 8 presents a comprehensive comparative TEA and GHG estimate of domestic ammonia production utilizing ATR-CCS-OC across 63 major countries. According to the TEA results in Fig. 8(a), production costs exhibit substantial variation, ranging from \$0.38 per $kgNH_3$ (Saudi Arabia, SA) to \$4.42 per $kgNH_3$ (Argentina, AR). (Note that, Venezuela, VE, exhibits exceptionally low FCR and fuel costs due to high inflation combined with relatively low risk-free rates and risk premiums, resulting in the lowest LCOA across most figures.) This regional analysis indicates that Middle Eastern nations achieve the lowest mean production costs at \$0.49 per $kgNH_3$, followed by North America (\$0.53 per $kgNH_3$), Asia-Pacific (\$0.63 per $kgNH_3$), South America (\$0.70 per $kgNH_3$), Africa (\$0.74 per $kgNH_3$), and Europe (\$0.78 per $kgNH_3$) excluding

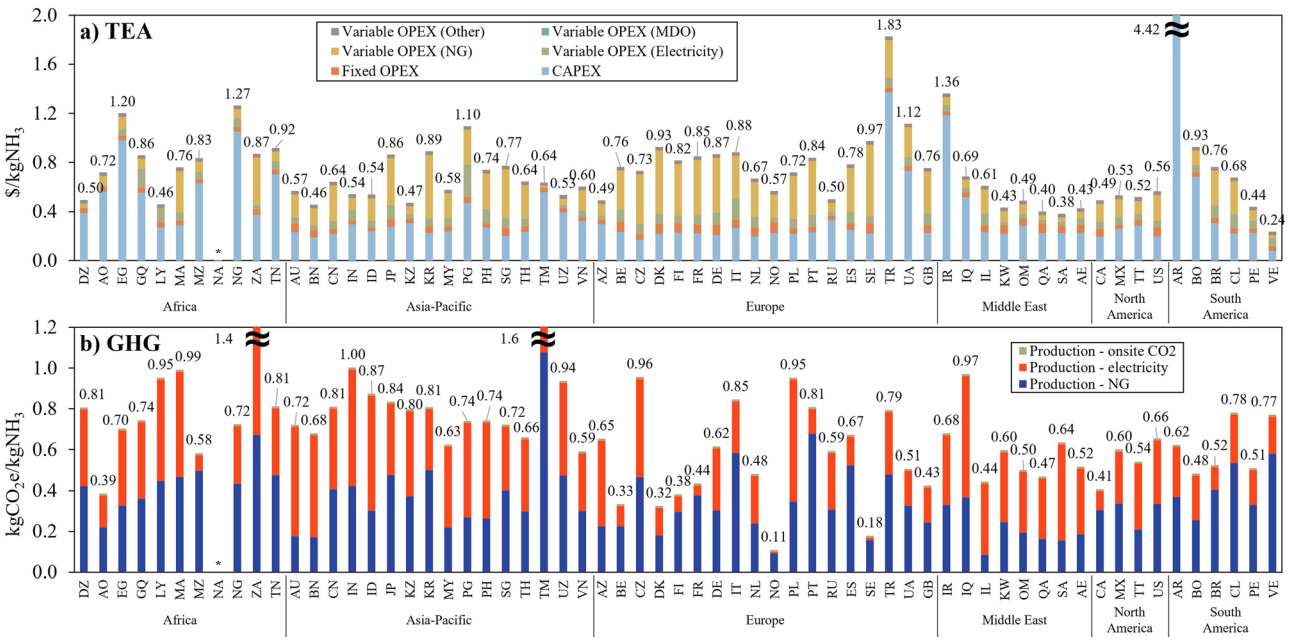

Fig. 8 (a) Cost and (b) GHG emissions of domestic NH_3 production: (a) TEA and (b) GHG results of ATR-CCS-OC.

extreme values. Cost structure reveals that CAPEX constitutes 22–87% (46% in average) of total production costs in most countries, with this substantial variation attributable to country-specific FCR (primarily due to WACC and inflation rates) and locational factors. Among variable operational expenditures, natural gas costs represent the most significant component, conferring economic advantages to countries with low natural gas prices ($1–3 per mmbtu) such as Middle Eastern nations and Russia. The notably low production costs in Qatar ($0.40 per kg$NH_3$), Saudi Arabia ($0.38 per kgNH_3), and the United Arab Emirates ($0.43 per kg$NH_3$) are primarily attributable to these competitive natural gas price. Conversely, European countries (excluding Azerbaijan, Norway, and Russia) and Asia-Pacific nations dependent on natural gas imports (*e.g.*, South Korea and Japan) demonstrate elevated production costs due to high natural gas prices ($8–20 per mmbtu). Financing costs further contribute to inter-country cost disparities. Egypt, Nigeria, Türkiye, Iran, and Argentina exhibit significant FCR (Fig. 3) due to the recent capital risk premiums, thereby incurring higher production costs relative to countries with more favorable financing conditions.

Life cycle GHG emission results in Fig. 8(b) reveal that GHG emissions from ATR-CCS-OC ammonia production exhibit a range from 0.11 kgCO_2e per kgNH_3 (Norway, NO) to 1.59 kgCO_2e per kgNH_3 (Turkmenistan, TM). Given the implementation of CCS, onsite CO_2 emissions are negligible; therefore, the emission results attributable to natural gas and electricity consumption correlate with country-specific upstream emission profiles. Inter-country variations in natural gas upstream emissions stem from differences in methane leakage during extraction, processing, and transportation, energy efficiency differentials, flaring rates, and the presence of additional processes for procurement (*e.g.*, liquefaction and LNG shipping) as detailed in Section 2.4 and SI. Similarly, grid electricity upstream emission disparities primarily derive from differences in power generation mix, upstream emissions of power plant's fuels, and transmission and distribution losses. This regional GHG emission analysis indicates that Asia-Pacific countries exhibit the highest average emissions at 0.82 kgCO_2e per kgNH_3. India (1.01 kgCO_2e per kgNH_3) and Indonesia (0.89 kgCO_2e per kgNH_3) demonstrate particularly elevated emissions due to carbon-intensive power generation mixes (predominantly coal-based). Turkmenistan (1.59 kgCO_2e per kgNH_3) shows the highest emission due to the extreme CH_4 leakage record in NG upstream processes. South Korea (0.81 kgCO_2e per kgNH_3) and Japan (0.84 kgCO_2e per kgNH_3) show high natural gas upstream emissions resulting from complex, energy-intensive LNG import processes associated with their import-dependent natural gas supply chains. European countries, by contrast, achieve comparatively lower mean emissions (0.56 kgCO_2e per kgNH_3), with Scandinavian nations such as Norway (0.11 kgCO_2e per kgNH_3), Finland (0.38 kgCO_2e per kgNH_3), and Sweden (0.18 kgCO_2e per kgNH_3) demonstrating superior environmental performance through efficient natural gas infrastructure and low-carbon power generation mixes. Russia (0.59 kgCO_2e per kgNH_3) exhibits favorable natural gas upstream emissions comparable to these Scandinavian countries, but its relatively less decarbonized power mix results in overall GHG emissions exceeding the European average. Notably, Middle Eastern countries, despite their economic advantages, demonstrate relatively high emission levels (average 0.60 kgCO_2e per kgNH_3). This is attributed to their predominantly fossil fuel-based power generation (natural gas and oil-based), which is a consequence of exceptionally low domestic fossil fuel prices relative to other countries.

Fig. 9 presents a comparative TEA and life cycle GHG emissions of electrolytic ammonia production utilizing LTE

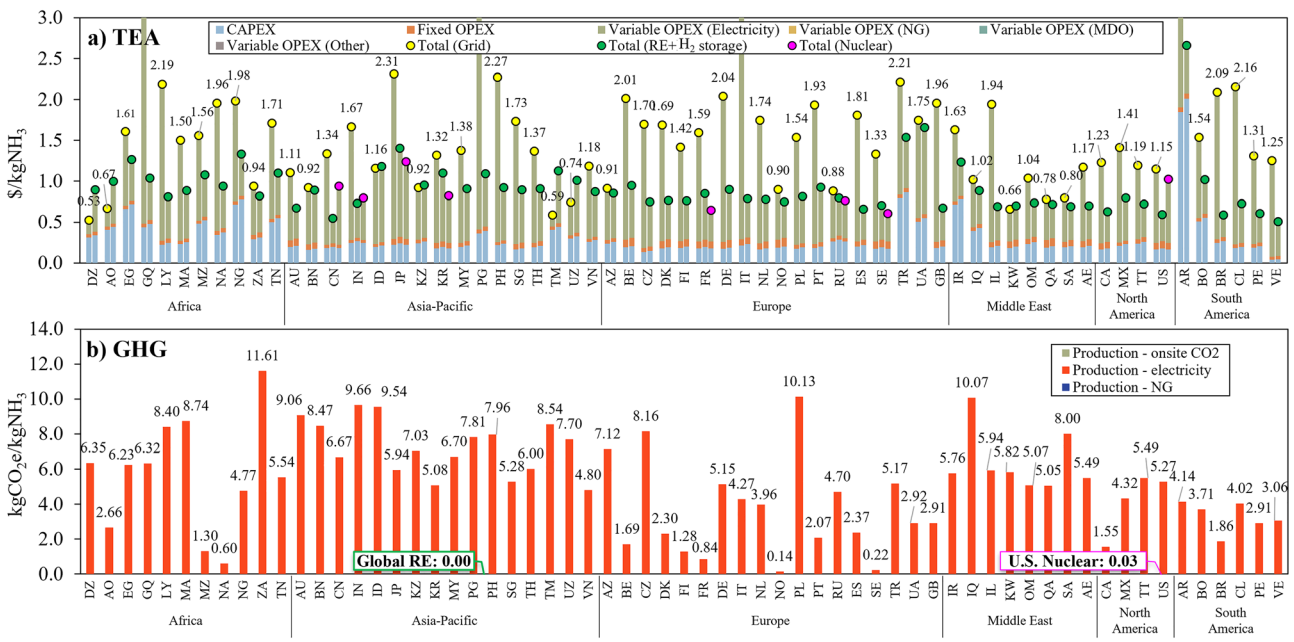

Fig. 9 (a) Cost and (b) GHG emissions of domestic NH_3 production: (a) TEA and (b) GHG result of LTE-grid, LTE-RE, LTE-nuclear.

across 63 countries. This analysis encompasses multiple production scenarios differentiated by electricity source: grid electricity, renewable energy with hydrogen storage, and nuclear power. As illustrated in Fig. 9(a), production costs for LTE-based electrolytic ammonia exhibit variation mainly contingent upon country-specific electricity prices and CAPEX impact. In the grid electricity utilization scenario (yellow circles), production costs range from \$0.53 per $kgNH_3$ (Algeria, DZ) to \$3.34 per $kgNH_3$ (Italia, IT). This regional analysis of yellow ammonia cost reveals geographical disparities, with average production costs of \$1.62 per $kgNH_3$ in Africa, \$1.56 per $kgNH_3$ in Asia-Pacific, \$1.71 per $kgNH_3$ in Europe, \$1.13 per $kgNH_3$ in the Middle East, \$1.25 per $kgNH_3$ in North America, and \$1.93 per $kgNH_3$ in South America. The Middle Eastern region demonstrates superior economic performance, primarily attributable to preferential grid electricity pricing policies. The nuclear power utilization scenario, maintaining equivalent ammonia plant capacity factors through co-location with nuclear facilities, was analyzed for countries with significant nuclear generation capacity: China, India, Japan, South Korea, France, Russia, Sweden, and the United States (pink circles). The results indicate that pink ammonia represents a more economically advantageous option compared to yellow ammonia in countries with nuclear generation costs lower than grid electricity prices, such as India, Japan, South Korea, France, and Sweden. For green ammonia production (green circles), which assumes, in this study, incorporating hydrogen storage tanks as buffer mechanisms to integrate variable renewable electricity generation into continuous ammonia synthesis processes, effectively converting intermittent power profiles into stable ammonia production (for detailed assumption, refer Section 3.5), production costs exhibit significant geographical variation ranging from \$0.55 per $kgNH_3$ (China, CN) to \$2.66 per $kgNH_3$ (Argentina, AR). Notably, except for some countries (DZ, AO, ID, KZ, TM, and KW), grid electricity-based production costs exceed renewable energy-based production costs in most nations, suggesting that dedicated renewable energy system deployment for green ammonia production may already represent an economically advantageous strategy across numerous regions. Within the green ammonia scenario, China (\$0.55 per $kgNH_3$), North America (\$0.68 per $kgNH_3$), and Middle Eastern countries (\$0.79 per $kgNH_3$) demonstrate low production costs, attributable to high-capacity factors due to favorable solar panel's global horizontal irradiance (GHI) values, economies of scale, and abundant renewable energy resources. Conversely, Asia-Pacific countries (mean \$0.95 per $kgNH_3$) and European nations (mean \$0.88 per $kgNH_3$) record relatively higher production costs, reflecting comparatively higher renewable electricity costs.

Life cycle GHG emission results presented in Fig. 9(b) demonstrate that GHG emission characteristics of ammonia production correlate directly with the carbon intensity of electricity sources, thus exhibiting dependence on country-specific power generation mixes. Except for certain European countries that have nearly achieved decarbonization (France, Norway, and Sweden), yellow ammonia exhibits substantially higher emissions compared to their blue ammonia carbon intensity. In the grid electricity scenario, emissions range from 0.14 $kgCO_2e$ per $kgNH_3$ (Norway, NO) to 11.61 $kgCO_2e$ per $kgNH_3$ (South Africa, ZA). Particularly in countries with high coal-fired power generation proportions, including India (9.66 $kgCO_2e$ per $kgNH_3$), Indonesia (9.54 $kgCO_2e$ per $kgNH_3$), Poland (10.13 $kgCO_2e$ per $kgNH_3$), and Australia (9.06 $kgCO_2e$ per $kgNH_3$), the grid electricity-based ammonia production generates approximately 4–5 times higher life cycle GHG emissions than conventional natural gas-based gray ammonia. Conversely, nations with substantial hydroelectric and nuclear power contributions, such as Norway (0.14 $kgCO_2e$ per $kgNH_3$), France (0.84 $kgCO_2e$ per $kgNH_3$), and Sweden (0.22 $kgCO_2e$ per $kgNH_3$), achieve relatively low emissions even when utilizing grid electricity, substantiating the critical importance of low-carbon power mixes for the environmental performance of electrolytic ammonia production. In the case of green ammonia, as the study's methodological assumptions, GHG emissions are 0.00 $kgCO_2e$ per $kgNH_3$ across all countries. This approach aligns with emission quantification frameworks for clean hydrogen and ammonia in major economies (*e.g.*, U.S. Clean Hydrogen Production Tax Credit (45V) guidelines, Korean Clean Hydrogen Certification System[63,64]), which consider upstream emissions from renewable energy as negligible. It should be noted, however, that accounting for embodied emissions would yield non-zero values. Nuclear-based production (*e.g.* U.S. nuclear case) achieves minimal emissions (0.03 $kgCO_2e$ per $kgNH_3$), reflecting the inherently low GHG emissions associated with nuclear power generation (0.003 $kgCO_2e$ per kWh[61]).

Comparative analysis of Fig. 8 and 9 enables cost and emission performance differentials between electrolytic ammonia and blue ammonia. From a cost perspective, blue ammonia generally demonstrates advantages over electrolytic ammonia (both grid-powered and dedicated VRE-powered scenarios) in most countries with moderate capital financing costs. However, this cost differential exhibits regional variability, with green ammonia demonstrating greater cost-effectiveness than blue ammonia in regions where renewable energy resources are comparatively more affordable and abundant than natural gas resources, including China, Finland, Spain, Sweden, the United Kingdom, and Brazil. With respect to emissions, renewable energy-based green ammonia (0.00 $kgCO_2e$ per $kgNH_3$) maintains absolute advantages over blue ammonia (0.11–1.01 $kgCO_2e$ per $kgNH_3$) across all countries. However, grid electricity-based electrolytic ammonia records higher emissions than even gray ammonia in numerous countries, indicating that clean electrolytic ammonia necessitates either dedicated utilization of low-carbon power sources (renewable or nuclear) or substantial decarbonization of grid electricity generation portfolios.

3.3. Overseas importation from different countries

This section presents cost and GHG emission comparison of different importation countries cases. Fig. 10 shows supply chain costs and GHG emissions associated with ammonia importation to Japan from diverse origin countries. This case study assumes ATR-CCS-OC based blue ammonia, grid electricity utilization across all processes, and MDO as shipping fuel,

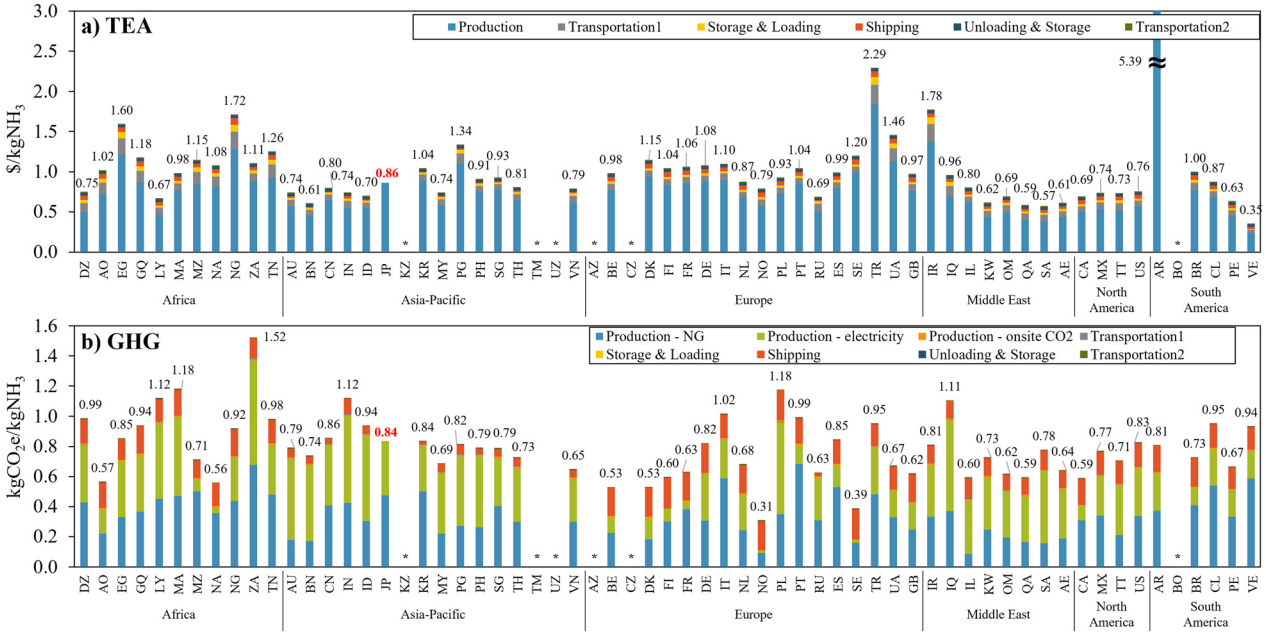

Fig. 10 (a) Cost and (b) GHG emissions overseas NH_3 importation (Japan target, ATR-CCS-OC, Grid, MDO, no reconversion). Domestically produced ammonia is expressed in red. Dot (*) indicates the landlocked country.

and the scope covers the entire supply chain from production to pre-reconversion stages. According to the TEA results illustrated in Fig. 10(a), ammonia importation costs to Japan demonstrate variation by the origin country. Production costs typically constitute the predominant component, accounting for approximately 67–86% of total LCOA. Countries characterized by exceptional FCR (Egypt, Nigeria, Türkiye, Iran, and Argentina) or high natural gas prices due to complicated NG procurement processes (South Korea) or exceptionally high grid pricing (Papua New Guinea), and most European countries excluding Northern Europe and Russia, exhibit markedly higher production costs. Conversely, the Middle East, Russia, North America, and Peru demonstrate competitive production costs attributable to moderate financing cost and favorable natural gas pricing structures. Maritime transportation and storage costs demonstrate proportional increases with the voyage distance between two countries, representing 6–20% of total costs. Proximate nations including South Korea ($0.07 per $kgNH_3$), China ($0.07 per $kgNH_3$), and Russia ($0.08 per $kgNH_3$) incur relatively minimal transportation expenditures, while the most distant countries in Northern Europe and South America generate transportation and storage costs of approximately $0.1–0.2 per $kgNH_3$. From an overall LCOA perspective, Middle Eastern nations offer the most competitive supply costs, averaging $0.69 per $kgNH_3$ except Iran, attributable to the advantageous combination of low production costs and moderate geographical positioning relative to Japan within the global supply network context. Additionally, Algeria, Libya, Brunei, Australia, Indonesia, Russia, North America, and Peru demonstrate favorable overall costs through either low production costs or geographical proximity advantages. Notably, when compared to domestic Japanese ammonia production costs ($0.86 per $kgNH_3$), importation from the above cost-effective countries shows approximately 20% more economical.

The life cycle GHG emission results presented in Fig. 10(b) demonstrate that the GHG emission performance of ammonia importation spans from 0.28 $kgCO_2e$ per $kgNH_3$ (Norway, NO) to 1.51 $kgCO_2e$ per $kgNH_3$ (South Africa, ZA). This variance primarily derives from country-specific differences in upstream emissions of natural gas and grid electricity during production stages, coupled with emission variations associated with the shipping stage. Shipping emissions demonstrate proportional increases with the voyage distance, ranging from 0.02 to 0.18 $kgCO_2e$ per $kgNH_3$, reflecting GHG emissions from both upstream processes and combustion of MDO shipping fuel. These emissions constitute particularly significant contributors to long-distance importation routes, such as those from European countries or South America. For total GHG emissions, European and Middle Eastern countries record relatively low emissions, averaging 0.69 and 0.72 $kgCO_2e$ per $kgNH_3$, respectively. The Middle Eastern region demonstrates particularly balanced performance across both economic and environmental dimensions, attributable to relatively moderate shipping distances to Asian markets resulting in moderate shipping costs and emissions, combined with favorable natural gas pricing and upstream emission profiles.

This analysis demonstrates that optimal source country selection requires integrating both production economics and environmental performance with distance-dependent logistical factors. For Japan specifically, Middle Eastern nations, Norway, Russia, and Canada emerge as superior trade partners, exhibiting advantageous performance across both cost and emission metrics under the specified technological parameters.

3.4. Overseas exportation to different countries

This section presents cost and GHG emission performance of different exportation country options. Fig. 11 shows total supply chain costs and GHG emissions associated with the exportation of U.S.-produced ammonia to diverse destination countries. This analysis assumes ATR-CCS-OC based blue ammonia, grid electricity utilization across all processes, and MDO as shipping fuel. The TEA results illustrated in Fig. 11(a) indicate that the total LCOA of U.S.-produced blue ammonia to various destination countries ranges from \$0.70 per $kgNH_3$ (Mexico, MX) to \$1.02 per $kgNH_3$ (Argentina, AR). This variability is notably lower than that observed in the importation scenario, primarily because the fixed production cost (\$0.56 per $kgNH_3$) establishes a stable baseline component for all exportation pathways. While production costs remain constant across all export routes, transportation, shipping, and storage-related expenditures constitute the principal variable components, ranging from \$0.12 to 0.45 per $kgNH_3$. Specifically, storage and shipping costs demonstrate proportional increases with voyage distances. Consequently, North American destinations (Canada: \$0.71 per $kgNH_3$, Mexico: \$0.70 per $kgNH_3$, Trinidad and Tobago: \$0.72 per $kgNH_3$) exhibit the lowest LCOA due to geographical proximity. European destinations record the second-lowest average costs at \$0.74 per $kgNH_3$, followed by Middle Eastern (\$0.76 per $kgNH_3$) and Asia-Pacific (\$0.76 per $kgNH_3$) regions, which demonstrate comparable cost profiles at the higher end of the spectrum.

The GHG emission results presented in Fig. 11(b) demonstrate range from 0.68 $kgCO_2e$ per $kgNH_3$ (Mexico) to 0.85 $kgCO_2e$ per $kgNH_3$ (Thailand, TH). This emission variability pattern proves as a function of maritime transportation distance, similar to the economic analysis. The strong positive correlation between economic and environmental performance across export destinations indicates that the geographical distance constitutes a dominant factor influencing both cost and emissions metrics, suggesting that cost-efficient export routes generally offer environmental advantages as well. However, the country-specific GHG emission results exhibit relatively lower variability compared to costs, as emission variability originates predominantly from shipping emissions, which maintain an approximately linear relationship with maritime transportation distances. Countries within the same geographical region demonstrate highly similar emission profiles, with inter-regional variability substantially exceeding intra-regional variability. Based on comparison with the domestic U.S. production emissions (0.66 $kgCO_2e$ per $kgNH_3$), all export pathways incur 2–21% additional emissions, indicating GHG reduction potential through maritime transport decarbonization or regional ammonia supply chain optimization.

Comparative cost analysis of specific country's domestic production costs *versus* import costs from diversified countries yields substantive market penetration implications. For instance, Saudi Arabia's domestic production costs (\$0.38 per $kgNH_3$, referenced in Fig. 8) render US imports (\$0.74 per $kgNH_3$) economically challenging for market penetration. Conversely, Japan and South Korea represent relatively competitive markets, with minimal differentials between domestic production costs (\$0.86 and 0.89 per $kgNH_3$, respectively) and US import costs (\$0.76 and 0.75 per $kgNH_3$, respectively). Similar patterns emerge in GHG emission considerations, with environmentally inefficient US imports (0.74 $kgCO_2e$ per $kgNH_3$) to low-emission production regions such as Norway (domestic: 0.11 $kgCO_2e$ per $kgNH_3$), while high-emission production regions like India (domestic: 1.00 $kgCO_2e$ per $kgNH_3$) demonstrate environmental advantages through US imports (0.82 $kgCO_2e$ per $kgNH_3$). These findings indicate that global ammonia trade flows will not simply follow theoretical total cost

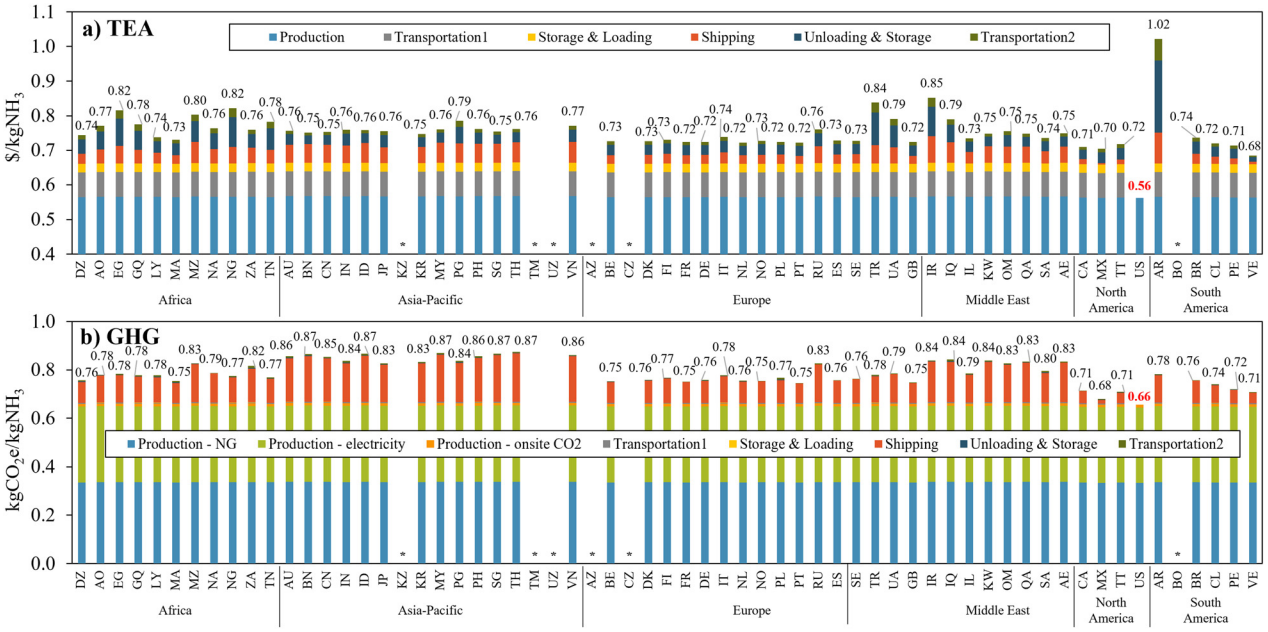

Fig. 11 (a) Cost and (b) GHG emissions overseas NH_3 exportation (U.S. origin, ATR-CCS-OC, Grid, MDO, no reconversion). Domestically produced ammonia is expressed in red. Dot (*) indicates the landlocked country.

or emission minimization pathways but will emerge from the complex interplay of country-specific production economics, regional supply–demand patterns, geographical transportation distances, and varying environmental priorities across different jurisdictions.

3.5. Inter-country cost and GHG emissions

Fig. 12–15 present comprehensive TEA and life cycle GHG emission matrix analysis of global blue and green ammonia trade dynamics. These matrices map the LCOA and life cycle GHG emissions across country-specific production-consumption pairs (origin–target pairs) through heat map visualization. The supplementary information (.xlsx format) provide detailed results and assumptions for the blue, green, gray, and yellow ammonia supply chains. This file includes the data presented in Fig. 12–16 (for blue and green ammonia) and also contains data on hydrogen supply chain costs and GHG emissions. Fig. 12 displays TEA results for blue ammonia (based on ATR-CCS-OC), while Fig. 13 presents life cycle GHG emission results. Fig. 14 shows TEA results for green ammonia (utilizing LTE with dedicated renewable electricity and

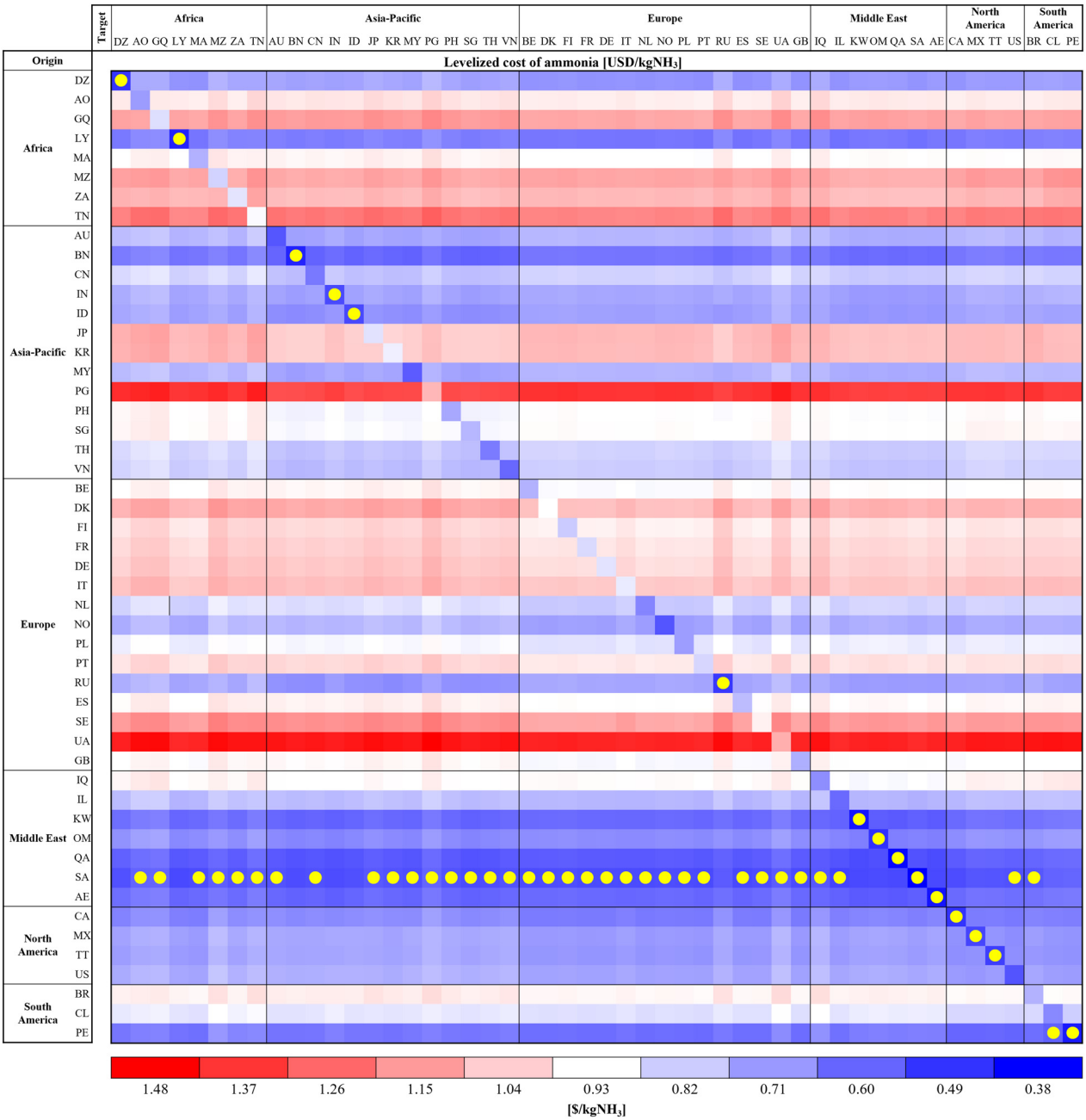

Fig. 12 Blue NH_3 inter-country cost [$ per $kgNH_3$]. Note that, EG, NA, NG, KZ, TM, UZ, AZ, CZ, BO, TR, IR, AR, and VE have been excluded for clearer visualization due to their out-ranged FCR, source availability, and their landlocked location. The diagonal line represents the domestic production cases. Yellow dot indicates the lowest origin country option for the corresponding target country.

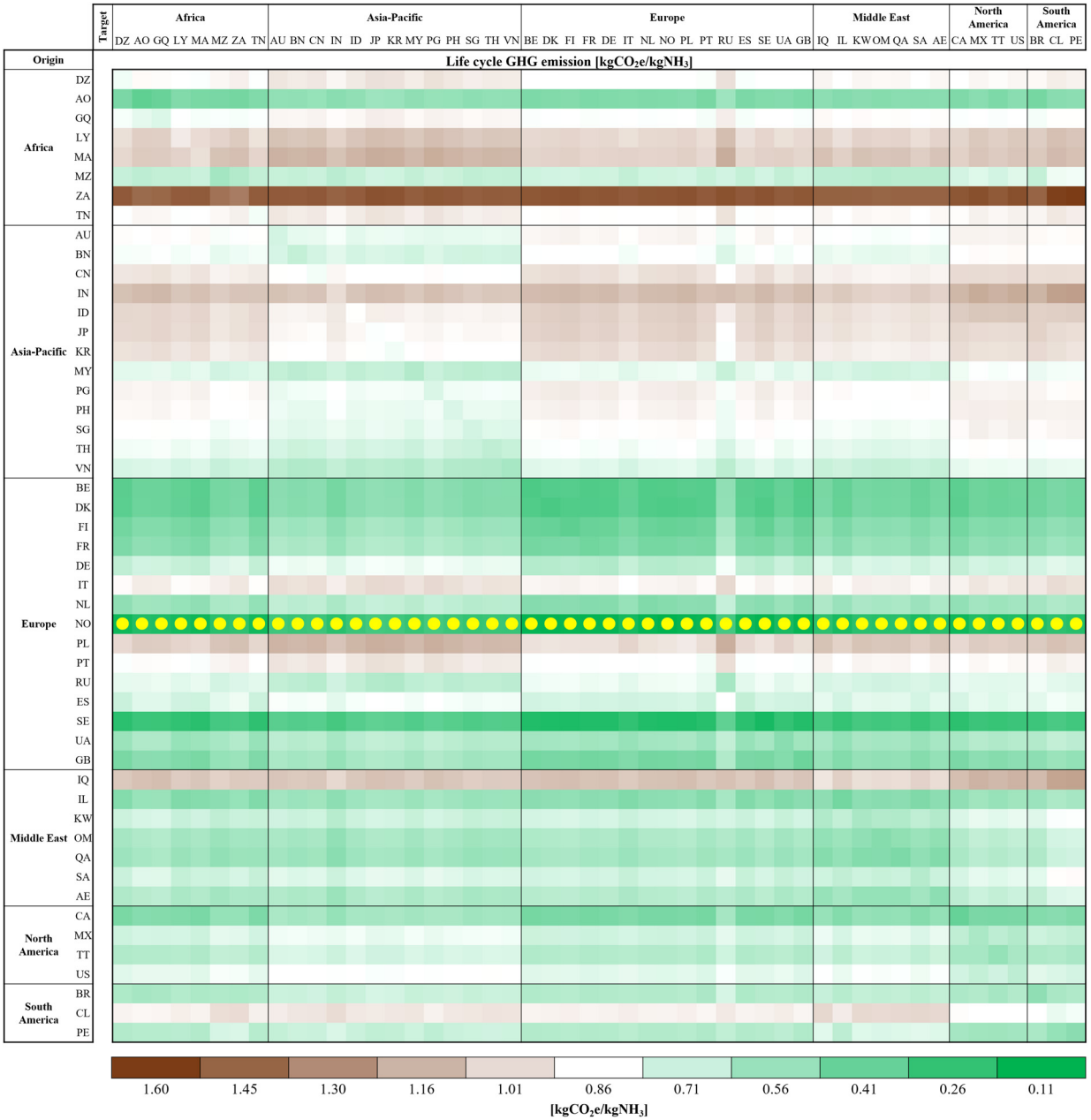

Fig. 13 Blue NH_3 inter-country emission [$kgCO_2e$ per $kgNH_3$]. Note that, EG, NA, NG, KZ, TM, UZ, AZ, CZ, BO, TR, IR, AR, and VE have been excluded for clearer visualization due to their out-ranged FCR, source availability, and their landlocked location. The diagonal line represents the domestic production cases. Yellow dot indicates the lowest origin country option for the corresponded target country.

hydrogen storage tank) and Fig. 15 shows the life cycle GHG emission results of the corresponding cases. The color gradients provide intuitive visualization of cost and emission metrics: in the LCOA matrix, blue indicates lower costs while red indicates higher costs; in the life cycle GHG matrix, green represents lower emissions while brown represents higher emissions. Yellow dots highlight the lowest-cost origination country option (row) for each corresponding destination country (column), and diagonal elements represent domestic production–consumption scenarios.

The blue ammonia cost matrix (Fig. 12) demonstrates substantial cost variability across supply chain routes, ranging from \$0.38 per $kgNH_3$ to \$1.48 per $kgNH_3$. Cost analysis reveals several structural patterns:

– Saudi Arabia (SA) emerges as the optimal supply country for numerous destination markets, with other Middle Eastern nations and Peru functioning as almost near optimal suppliers. These countries demonstrate cost advantages for North Africa (excluding Morocco and Algeria), Asia-Pacific (excluding Brunei, India, Indonesia), Europe (excluding Russia), United States, and Brazil.

– Diagonal elements (domestic production case) record as optimal options within their procurement options for major

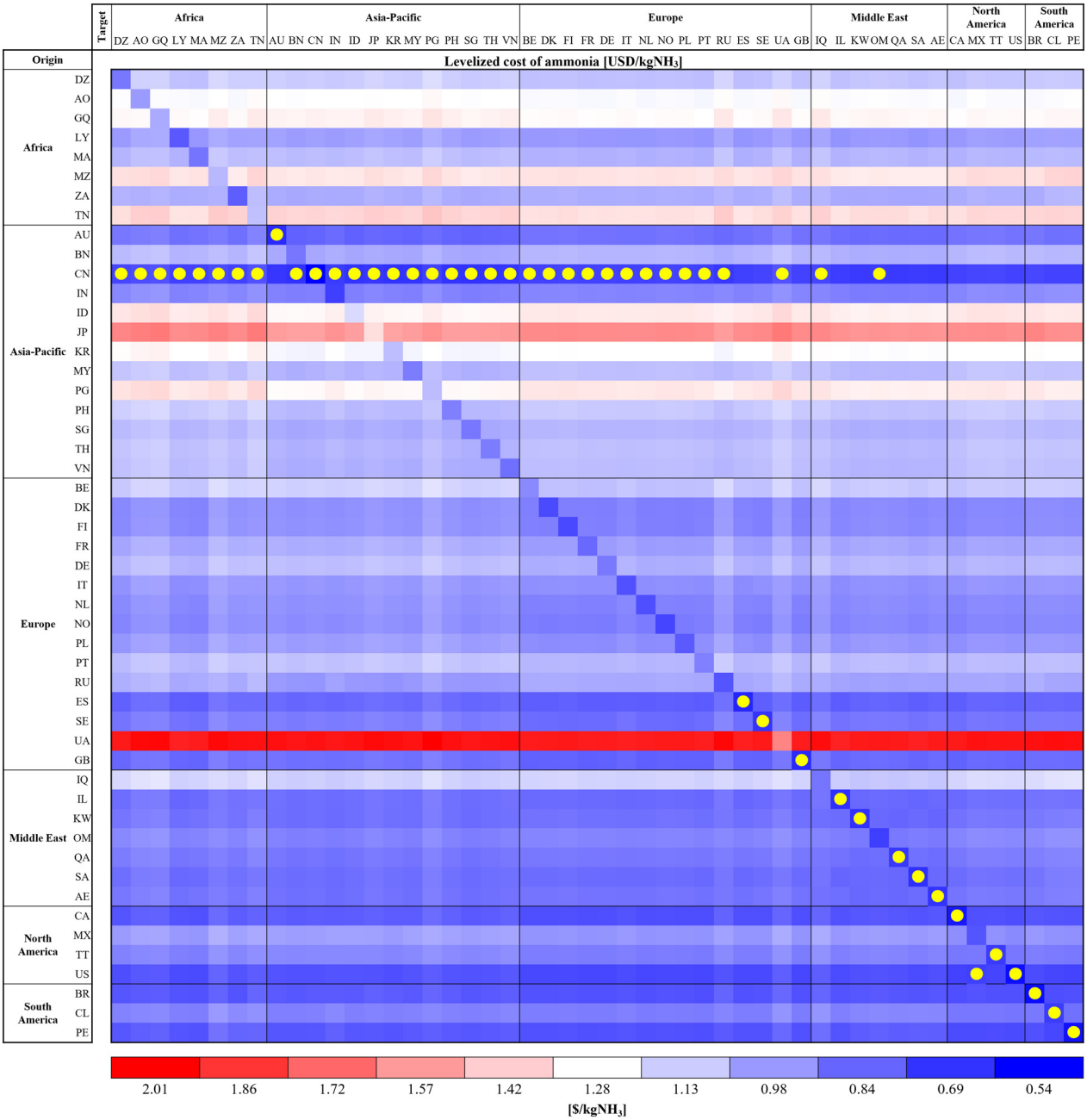

Fig. 14 Green NH_3 inter-country cost [$ per $kgNH_3$]. Note that, EG, NA, NG, KZ, TM, UZ, AZ, CZ, BO, TR, IR, AR, and VE have been excluded for clearer visualization due to their out-ranged FCR, source availability, and their landlocked location. The diagonal line represents the domestic production cases. Yellow dot indicates the lowest origin country option for the corresponding target country.

natural gas-abundant countries (*e.g.*, Algeria, Libya, Brunei, Indonesia, India, Russia, Middle East countries, Canada, Mexico, Trinidad and Tobago, and Peru). This indicates that domestic production and consumption in these countries presents economic advantages over blue ammonia importation. Conversely, numerous countries demonstrate greater economic efficiency through importation rather than domestic production.

– Supply routes originating from some Africa (GQ, MZ, ZA, and TN), and LNG-importing Asia-Pacific (JP and KR), and PG (having high grid price), and most of the Europe (except Northern Europe and Russia) exhibit higher production costs. This non-competitive cost structure derives from excessive production costs attributable to high natural gas and electricity prices in these countries of origin.

– Traditional natural gas producing countries generally demonstrate cost efficiency (blue coloration) within their respective regions, potentially indicating cost advantages as prospective regional blue ammonia suppliers.

The blue ammonia GHG emission matrix (Fig. 13) exhibits variability within the range of 0.11–1.58 $kgCO_2e$ per $kgNH_3$.

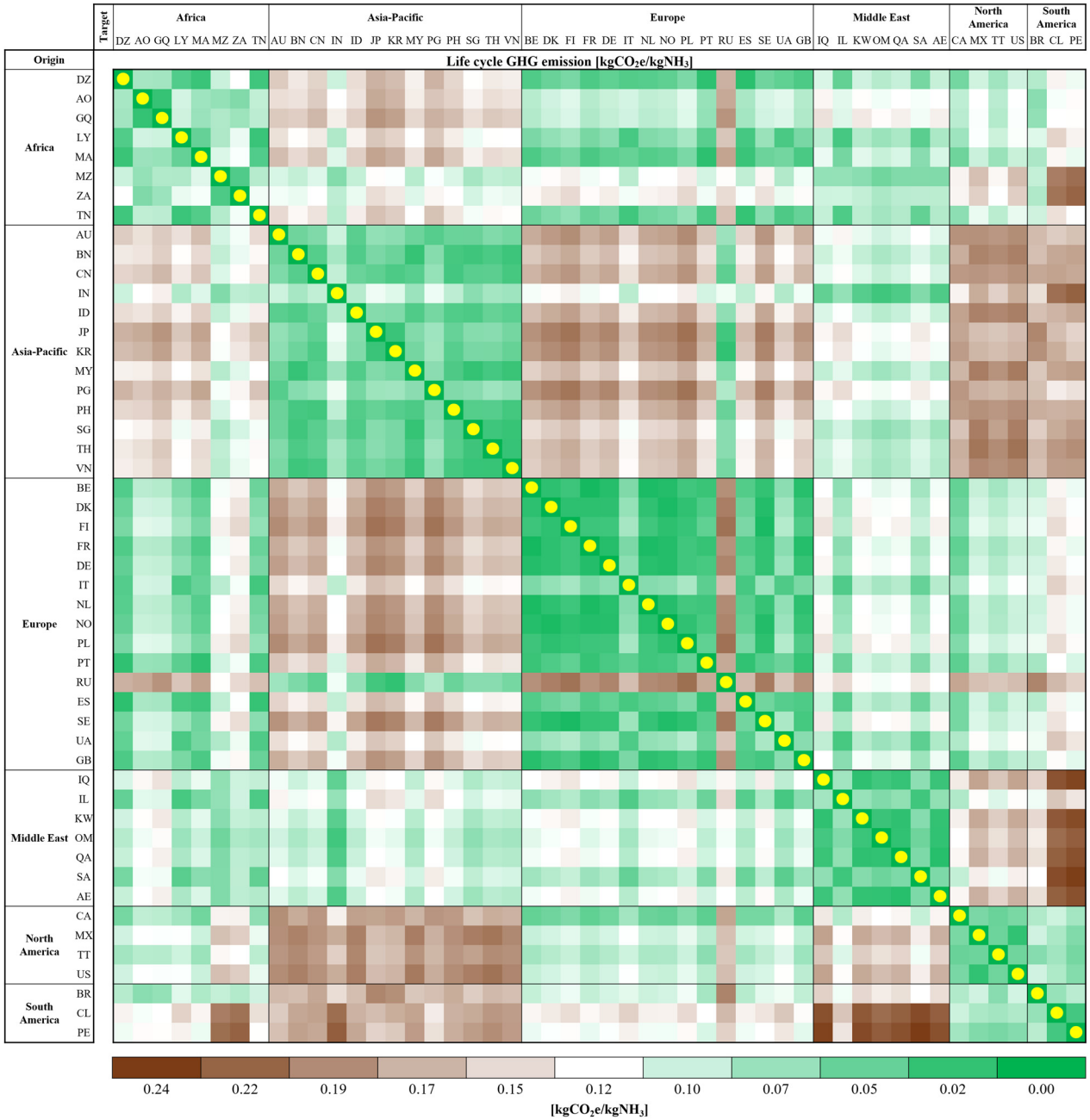

Fig. 15 Green NH_3 inter-country emission [$kgCO_2e$ per $kgNH_3$]. Note that, EG, NA, NG, KZ, TM, UZ, AZ, CZ, BO, TR, IR, AR, and VE have been excluded for clearer visualization due to their out-ranged FCR, source availability, and their landlocked location. The diagonal line represents the domestic production cases. Yellow dot indicates the lowest origin country option for the corresponding target country.

Notable characteristics in the distribution of emissions include:

– Norway (NO) records minimum GHG emission options across all destination countries. This advantage derives from efficient NG upstream processes, low methane leakage resulting in low upstream emissions, and a predominantly renewable grid yielding minimal electricity upstream emissions. Finland, Sweden, and Canada demonstrate similar emission options for target countries.

– Most Asia-Pacific countries exhibit non-favorable emission characteristics as origins. Consequently, blue ammonia produced within these regions represents a relatively high-emission option within global supply chains.

The green ammonia cost matrix (Fig. 14) exhibits a range from \$0.54 per $kgNH_3$ to \$2.01 per $kgNH_3$. Several structural patterns characterize the green ammonia cost distribution:

– China emerges as an optimal supply country for destination markets excluding other renewable electricity abundant countries such as Australia, Sweden, Spain, United Kingdom, most of the Middle Eastern countries and North and South America. This competitive advantage derives from comparatively low renewable LCOE. This pattern indicates that China

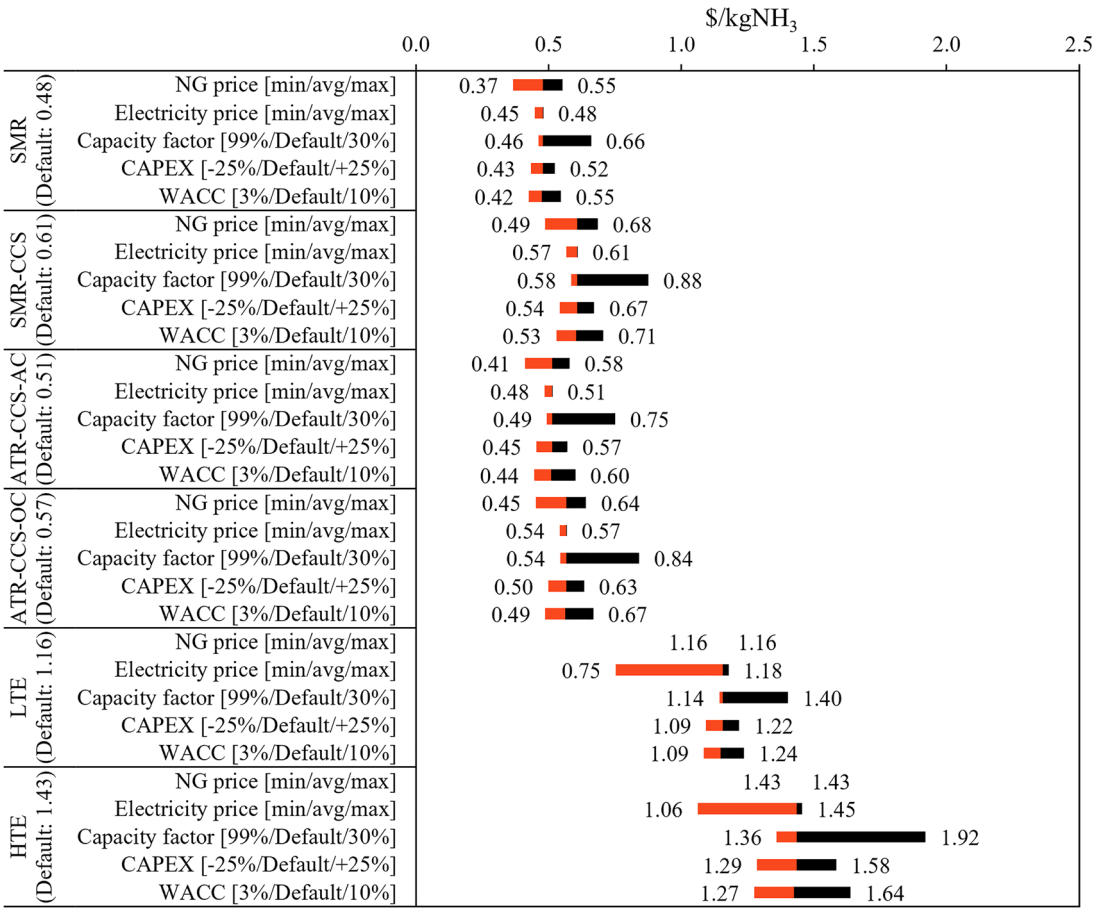

Fig. 16 Sensitivity of key TEA parameters to LCOA. Assumed US production and 100 tonnes NH_3 per h scenario.

can be the strongest competitiveness for green ammonia, and the Middle Eastern region maintains global competitiveness across both low-carbon (blue and green) ammonia pathways.

– Conversely, Indonesia, Japan, South Korea, Papua New Guinea, and Ukraine exhibit substantially higher supply costs as origin countries, reflecting substantial renewable LCOE attributable to constrained renewable resources, lower capacity factors, and related capital expenditures. Consequently, these nations demonstrate greater economic efficiency through importation rather than domestic production of green ammonia.

– The green ammonia cost matrix displays more distinct regional clustering patterns compared to blue ammonia, reflecting geographical correlations in renewable energy resource conditions (including capacity factors).

The green ammonia emission matrix (Fig. 15) demonstrates the range of 0.00–0.21 $kgCO_2e$ per $kgNH_3$, substantially lower than blue ammonia emissions. Key characteristics of the green ammonia emission matrix include:

– Diagonal elements uniformly record 0.00 $kgCO_2e$ per $kgNH_3$, reflecting zero emissions because power consumption of the production is solely based on renewable electricity. Consequently, domestic production represents the optimal option for each country from a GHG emission perspective.

– WTP emissions increase proportionally with the geographical distance as they originate exclusively from transportation, storage, and shipping stages. Therefore, proximate intra-regional trade (*e.g.*, within Asia-Pacific and within Europe) demonstrates low emissions, while inter-continental long-distance trade (*e.g.*, Asia Pacific-Europe and Middle East-South America) records comparatively higher emissions.

– While GHG comparisons across green ammonia supply routes indicate that shorter-distance routes yield lower emissions, it is important to note that the magnitude of this variability is substantially less than that in blue ammonia scenarios.

3.6. Sensitivity and scenario analysis

This section presents a sensitivity analysis of key parameters and scenarios influencing costs and GHG emissions of the ammonia production process. Fig. 16 and 17 illustrate the sensitivity of LCOA and GHG emission across various ammonia production technologies, while Fig. 18 demonstrates the economic potential of diverse ammonia production pathways under various renewable power integration scenarios. Detailed quantitative assumptions for each case are comprehensively provided in the SI.

Fig. 16 depicts the sensitivity of key economic parameters across multiple ammonia production technologies (SMR, SMR-CCS, ATR-CCS-AC, ATR-CCS-OC, LTE, and HTE). For each technology, the analysis quantifies the impact of variations in natural gas prices, electricity prices, capacity factors, CAPEX, and WACC on the LCOAs, revealing several distinctive characteristics. Note that the natural gas and electricity price ranges reflect historical market price changes, incorporating both the lowest and highest price points observed over the past two decades. For conventional SMR, natural gas price variations within the range of \$3.2(minimum)–\$6.9(default)–\$9.3(maximum) per mmbtu-LHV demonstrate the most significant impact on LCOA compared to other parameters. This predominant influence derives from natural gas functioning as both the primary feedstock and energy source in the SMR process. Conversely, electricity price variance (\$46 (minimum)–\$83(default)–\$85(maximum) MW^{-1} h^{-1}) and CAPEX variations (±25%) exhibit relatively constrained impacts, attributable to minimal electricity consumption and comparatively low CAPEX contribution on total LCOA in SMR processes. For carbon capture-equipped technologies (SMR-CCS, ATR-CCS-AC, and ATR-CCS-OC), while natural gas price remains the one of the dominant influencing factors, capacity factors demonstrate significantly higher sensitivity compared to conventional SMR. The lower bound of the capacity factor variation range (30–99%) contemplates scenarios where VRE sources such as solar or wind facilities are dedicated to plant operations, potentially limiting the ammonia production facility's capacity factor to that of the power generation facility. The amplified capacity factor sensitivity in blue ammonia pathways relative to gray ammonia stems from their higher CAPEX proportion, which magnifies the impact of capacity factor on levelized costs. For LTE, electricity price sensitivity (\$0.75–1.18 per $kgNH_3$) and capacity factor sensitivity (\$1.14–1.40 per $kgNH_3$) emerge as the two most significant sensitivity factors, reflecting the predominant contribution of electricity costs and CAPEX to LCOA. It should be noted that this study assumes a relatively progressive PEM electrolyzer stack cost (\$460 per kW) based on NETL research.[71] However, alternative studies have employed substantially higher stack costs of up to \$1500 per kW for LTE,[72] which would increase CAPEX by approximately 240% relative to default assumptions. Such CAPEX variation could potentially elevate LCOA from \$1.16 per $kgNH_3$ to a maximum of \$2.35 per $kgNH_3$. HTE exhibits electricity price and capacity factor sensitivity patterns similar to LTE. From a CAPEX perspective, while this study assumes a stack cost of \$520 kW^{-1} for HTE,[71] some studies utilize values up to \$1700 per kW,[72] which would increase CAPEX by approximately 220% and potentially elevate LCOA from \$1.43 per $kgNH_3$ to a maximum of \$3.24 per $kgNH_3$. Notably, HTE demonstrates particularly pronounced sensitivity to capacity factors and WACC variations, attributable to the substantial contribution of capital costs to LCOA relative to other technological pathways, stemming from its expensive stack costs and replacement expenditures.

Fig. 17 presents sensitivity analysis results for key parameters to life cycle GHG emission profiles of the six ammonia production pathways, with parameters focused on upstream emission factors for natural gas and electricity. Note that both upstream emissions are normalized to emissions per one kWh, enabling a fair comparison between the different energy sources. For conventional SMR, variations of ±0.1 $kgCO_2e$/3.6MJ-LHV in natural gas upstream emission factors change total emissions within a range of ±0.05 $kgCO_2e$ per $kgNH_3$. Carbon capture-equipped technologies (SMR-CCS, ATR-CCS-AC, and ATR-CCS-OC) demonstrate natural gas upstream emission sensitivities comparable to conventional SMR. The impact

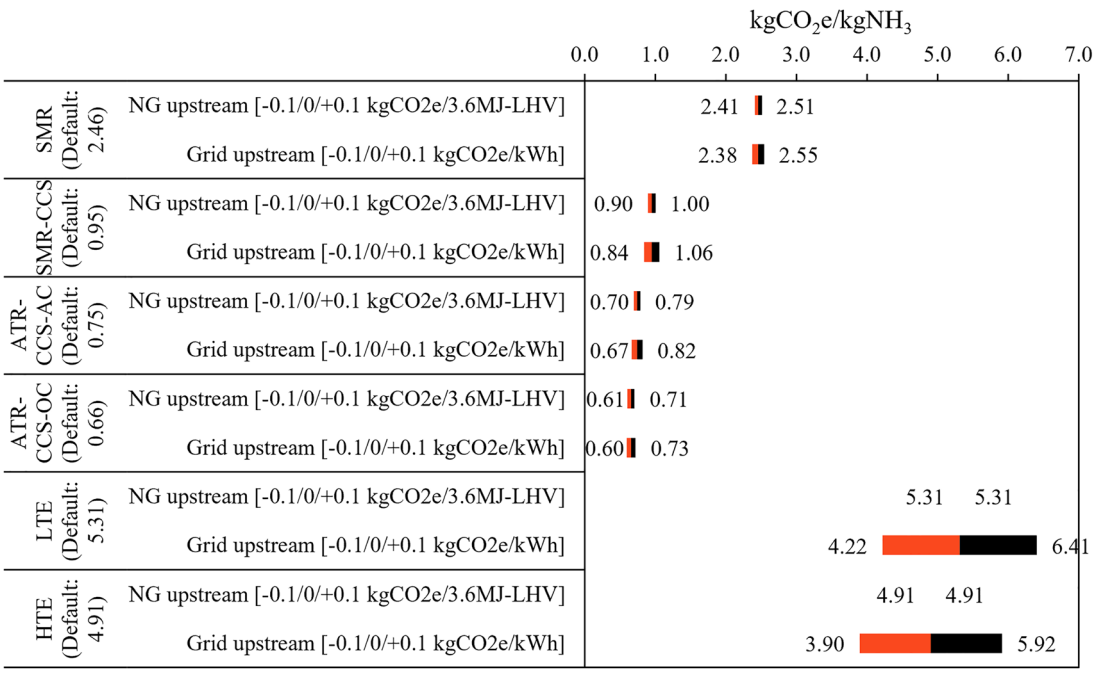

Fig. 17 Sensitivity of key GHG parameters to life cycle GHG emission. Assumed US production and 100 tonnes NH_3 per h scenario.

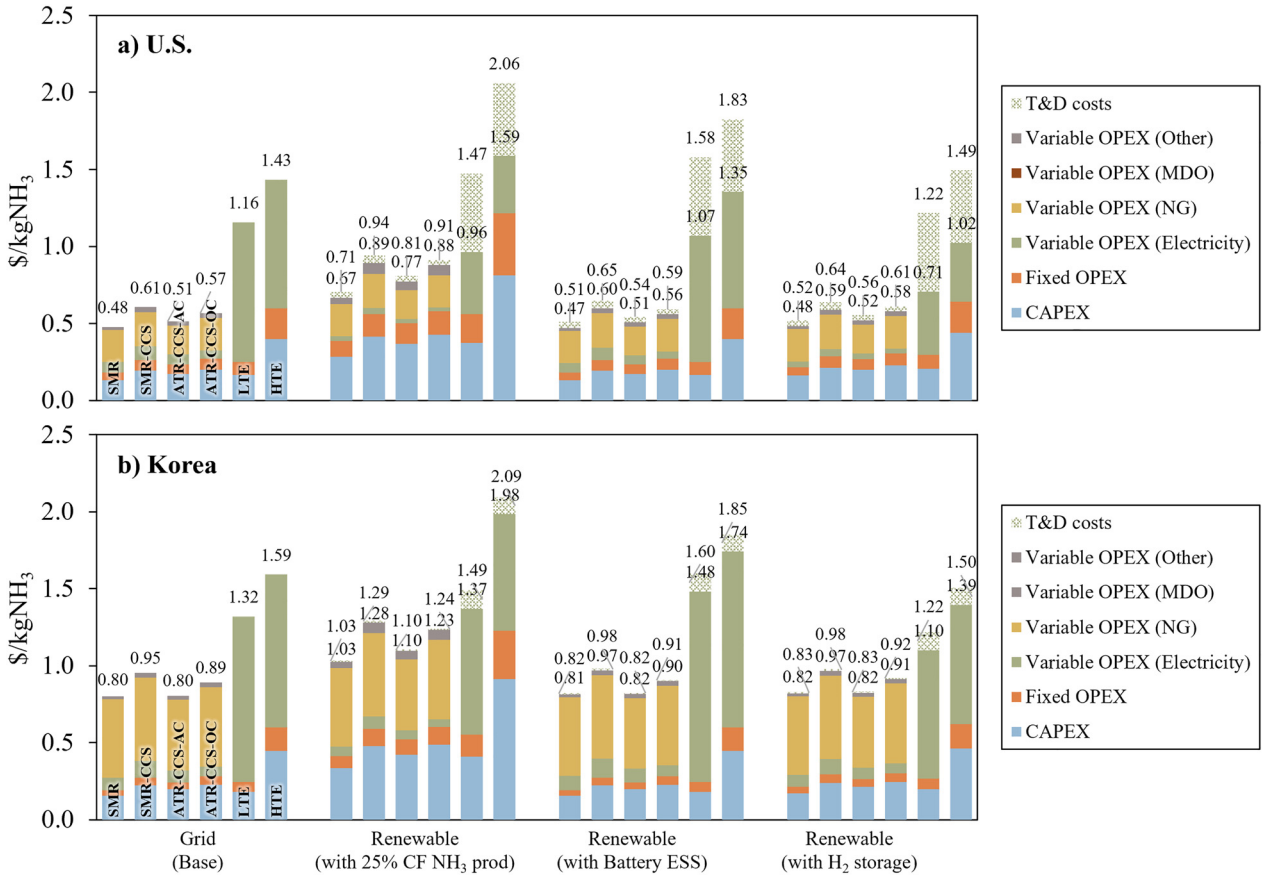

Fig. 18 Impact of the electricity source and integration scenario on LCOA and life cycle GHG emission: (a) US case and (b) South Korea case studies.

of grid electricity upstream emissions (±0.1 $kgCO_2e$ per kWh) varies across technologies: SMR (±0.08 $kgCO_2e$ per $kgNH_3$), SMR-CCS (±0.11 $kgCO_2e$ per $kgNH_3$), ATR-CCS-AC (±0.08 $kgCO_2e$ per $kgNH_3$), and ATR-CCS-OC (±0.06 $kgCO_2e$ per $kgNH_3$). These differential impacts reflect variations in electricity requirements per unit of ammonia production, with ATR-CCS-OC demonstrating the lowest and SMR-CCS the highest. This variability stems from two primary factors: first, the ATR-CCS-OC process achieves superior thermal efficiency through ASU unit process integration, enabling utilization of both oxygen and nitrogen byproducts as reformer gas and Haber–Bosch feedstock, respectively; second, the higher CO_2 concentration in ATR syngas requires less thermal and electrical energy for CCS facilities compared to SMR-based processes. Emissions from electrolysis technologies (LTE and HTE) depend exclusively on electricity upstream emissions. For LTE, variations of ±0.1 $kgCO_2e$ per kWh in grid electricity upstream emission factors modify total emissions within a range of 4.19–6.36 $kgCO_2e$ per $kgNH_3$, while HTE varies within 3.87–5.87 $kgCO_2e$ per $kgNH_3$. HTE demonstrates marginally lower sensitivity to grid electricity upstream emissions due to its superior energy efficiency. Nevertheless, both electrolysis technologies exhibit markedly higher sensitivity to electricity upstream emission than fossil fuel-based technologies.

Fig. 18 presents a comparative case study of LCOA across diverse production technologies and electricity supply scenarios, focusing on the United States (a) and South Korea (b). These two countries were selected as illustrative archetypes to represent contrasting national energy conditions: the U.S. as a nation with abundant, low-cost energy resources (*e.g.*, natural gas and renewables) and South Korea as a nation heavily reliant on energy imports with high renewable power generation costs. This analysis encompasses the six production technologies integrated with four distinct electricity supply scenarios: grid-powered, dedicated renewable (25% capacity factor), dedicated renewable with battery ESS, and dedicated renewable with a hydrogen storage tank. Through this high-contrast analysis, the study offers the economic performance of potential ammonia pathways under varying national conditions and scenarios.

In the United States context (Fig. 18(a)), if US averaged electricity transmission and distribution (T&D) costs are considered, all production technologies demonstrate higher LCOA results across all three renewable electricity scenarios compared to the baseline grid electricity scenario. However, in scenarios where dedicated renewable electricity sources are situated in close proximity to production facilities—thereby minimizing T&D costs to negligible levels—the economic advantages shift significantly, with optimal pricing outcomes varying according to the specific production technology and scenario parameters. The 25% capacity factor scenario, which simulates ammonia production facilities operating at capacity factors at 25%, which is equivalent to the higher bound of

VRE's capacity factor, exhibits approximately doubled CAPEX contribution to LCOA across all six production pathways compared to the grid scenario. When renewable electricity generators are dedicated to ammonia production plants, without power T&D cost considerations, the LTE scenario achieves an LCOA of \$0.96 $kgNH_3$, representing a cost reduction compared to the grid scenario (\$1.16 per $kgNH_3$). This economic advantage stems from the differential between grid electricity procurement costs (\$83 per MWh) and direct renewable electricity generation costs (\$29 per MWh) in the United States.[57,58,70] The battery ESS scenario, which incorporates sufficient battery capacity to transform intermittent renewable generation into firm power profiles to maintain high ammonia plant capacity factor, preserves the CAPEX contribution to LCOA at baseline levels. However, while the integration of battery ESS introduces an incremental increase (\$38.4 per MWh addition[73]) in the levelized cost of storage (LCOS), thereby elevating electricity procurement costs, this configuration still maintains economic superiority over grid-connected alternatives when T&D costs are excluded.

Among renewable electricity integration scenarios, the battery ESS configuration demonstrates the lowest cost outcomes for natural gas-based ammonia pathways. But the hydrogen storage tank scenario shows the lowest cost profiles for electrolysis-based ammonia pathways. The hydrogen storage tank scenario integrates hydrogen storage tank buffer to enable stable Haber–Bosch process operation while using VRE for hydrogen production, assuming additional \$350 per kgH_2 unit CAPEX and 214 kWh per $tonNH_3$ electricity consumption.[36] In this scenario, LTE and HTE achieve LCOA ranges of \$0.71–1.22 per $kgNH_3$ and \$1.02–1.49 per $kgNH_3$, respectively, demonstrating 29–39% economic advantages over grid electricity scenarios when T&D costs are excluded. However, when T&D costs are considered, all these pathways exhibit higher LCOA compared to grid electricity scenarios.

For the South Korea case, overall LCOA substantially exceeds those observed in the United States, attributable to higher energy prices (natural gas: \$17 per MMBtu, grid electricity: \$99 per MWh, renewable electricity: \$75 per MWh. See details in the SI). In the grid-based scenario, while SMR (\$0.80 per $kgNH_3$) maintains its position as the lowest-cost production pathway, its LCOA exceeds the corresponding US value by 67%. CCS-integrated pathways demonstrate approximately 56% higher cost levels compared to US equivalents, while LTE and HTE exhibit 11–13% cost premiums. Cost increments associated with renewable electricity integration are more pronounced in the South Korean context. In the 25% capacity factor scenario, all technology pathways demonstrate higher costs even when excluding T&D considerations. The battery ESS scenario exhibits particularly substantial cost escalation, with LTE and HTE achieving exceptionally high LCOA values of approximately \$1.48–1.60 per $kgNH_3$ and \$1.74–1.85 per $kgNH_3$, respectively. Consistent with US findings, the hydrogen storage scenario delivers the lowest cost outcomes for LTE/HTE pathways among the three renewable electricity integration scenarios. Moreover, South Korea exhibits lower T&D costs compared to the United States, resulting in the hydrogen storage tank scenario demonstrating approximately 6–8% lower electrolytic ammonia costs than the baseline grid electricity scenario, even when accounting for T&D costs.

Through comparative analysis of US and South Korean cases, this study confirms that the economic dynamics of integrating intermittent renewable electricity with ammonia production technologies demonstrate significant dependence on national energy market characteristics. Economic viability is determined by the complex interaction of several critical factors: (1) national grid electricity prices, (2) renewable electricity generation costs, (3) energy transmission and distribution cost structures, and (4) capital costs of electricity and hydrogen storage systems. The results particularly emphasize the importance of regional differentiation. Countries characterized by abundant renewable resources and low generation costs, such as China and Middle Eastern nations, may achieve economically competitive green ammonia production even when incorporating energy storage or hydrogen storage systems to mitigate the intermittencies. Conversely, in countries with constrained renewable resources and comparatively high generation costs, such as South Korea and Japan, green ammonia may remain economically disadvantaged relative to yellow ammonia utilizing grid electricity, even using analogous storage technologies. This global differentiation indicates that ammonia supply chain decarbonization strategies should be optimized by carefully considering each country's specific energy system costs, distribution characteristics, and the resulting cost and emission mapping data.

3.7. Implications on the global supply chain

This section quantitatively analyzes the potential cost and GHG impacts on the global ammonia supply chain resulting from future decarbonization pathways, utilizing the cost and greenhouse gas emission database developed in this study. For this analysis, the flow data of the global ammonia supply chain was aggregated from 2022 international ammonia trade data[11] and production data.[74] Total supply chain costs and GHG emissions were derived by applying the cost and GHG emission intensity database for various pathways to this flow data. 12 distinct pathway configurations were established: the current configuration (100% gray ammonia production and maritime transport using conventional MDO), and the other 11 decarbonizing combinations of varying adoption rates for low-carbon production technologies (blue/green) and shipping fuels (100% MDO/utilizing ammonia boil-off/100% ammonia cargo). The results for the total annual cost and GHG emissions of the global ammonia supply chain for each pathway are presented in Fig. 19.

Fig. 19(a) illustrates the relationship between the total annual GHG emissions and total costs for the global supply chain under the possible future pathways involving low-carbon production options and ammonia-fueled shipping options. The figure clearly presents the trade-off between cost and emissions associated with shifts in these options.

As discussed previously, blue and green productions exhibit higher costs than conventional gray in most regions. Consequently, transitioning the 100% gray, current configuration

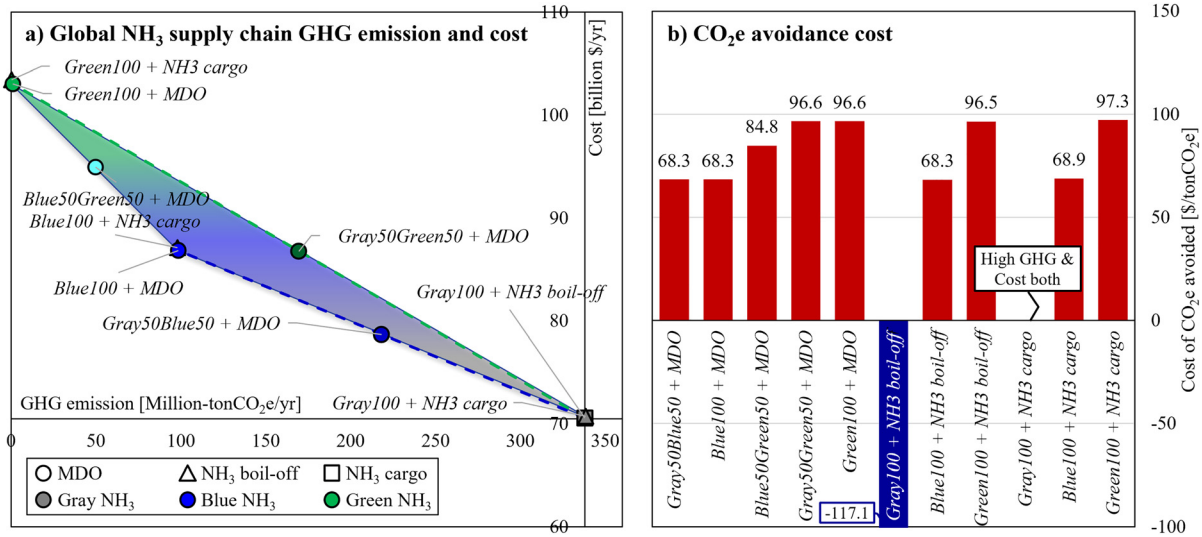

Fig. 19 Impact of decarbonization pathways on global ammonia supply chain's (a) total GHG emission and cost and (b) CO_2e avoidance cost. (Note for (a): the baseline point represents the current configuration's GHG emission (338.0 million tonneCO_2e per year) and cost ($70.6 billion per year). The colored triangle indicates the decarbonization frontier achievable with these options.)

(338.0 million tonneCO_2e per year and $70.6 billion per year) to 100% blue or 100% green results in total supply chain GHG emissions of 98.4 million tonneCO_2e per year and 1.0 million tonneCO_2e per year, respectively, with corresponding total costs of $87.0 billion per year and $103.1 billion per year. Between the two low-carbon routes, blue achieves a smaller cost increase per unit of abatement, which is consistent with the slope of the dashed trend lines in Fig. 19a) and with the cost of CO_2e avoidance (COA) in Fig. 19b) ($68.3 per tonne$CO_2e$ for blue and $ 96.6 per tCO_2e for green). Note that COA defined relative to the current configuration. In percentage terms, converting the gray-based current supply chain to blue or green raises total cost by 23.2% and 46.0%, while reducing GHG emissions by 70.9% and 99.7%, respectively.

Replacing a portion of MDO with NH_3 boil-off delivers dual benefits: about 0.08 million tonneCO_2e per year lower GHG emissions and $10 million per year lower total cost; the implied avoidance cost is negative. By contrast, using NH_3 cargo-as-fuel exhibits mixed outcomes that depend on the upstream NH_3 carbon intensity and price of ammonia at the origin. With gray ammonia, both emissions and cost increase (338.5 million tonneCO_2e per year, $70.7 billion per year). With blue, totals become 97.9 million tonneCO_2e per year and $87.1 billion per year; with green, 1.0 million tonneCO_2e per year and $103.1 billion per year. Therefore, utilizing NH_3 boil-off as ship fuel consistently offers both cost savings and GHG reductions compared to using 100% MDO. Conversely, using NH_3 cargo-as-fuel proves disadvantageous for gray ammonia, as both GHG and costs increase. For low-carbon ammonia, however, using NH_3 cargo reduces life cycle GHG emissions but entails a cost increase. This is attributed to the cargo ammonia used as ship fuel being a more expensive fuel than MDO ($9.2 per GJ-LHV) across most corridors.

4. Conclusion

This study conducted integrated techno-economic and life cycle GHG emissions of ammonia production routes (gray, blue, green, yellow, and pink) and downstream global supply chains across 63 major and emerging ammonia-producing, importing, and exporting countries. By providing cost and carbon-intensity results on a global scale, it offers a comprehensive dataset and methodology for evaluating ammonia's potential role as an international energy carrier. The analysis integrates extensive data on current and future production technologies, transportation, storage, and reconversion processes into the largest database to date for jointly examining economic and environmental factors in ammonia supply chains. In particular, we confirm that region-specific combinations of natural gas and electricity prices, upstream GHG emission profiles, capital costs (especially financing costs and location factors), and maritime transport distances can yield large variations in both levelized cost of ammonia and GHG emission profiles.

A comparative analysis of different production pathways and regional contexts reveals several key findings. First, conventional SMR-based production generally exhibits the lowest production cost (*e.g.*, $0.48 per kg$NH_3$ in the United States context) but also the highest direct GHG emissions (*e.g.*, 2.46 kgCO_2e per kgNH_3). Among blue ammonia pathways (SMR-CCS, ATR-CCS-OC, and ATR-CCS-AC), lowest achievable CO_2 avoidance cost among these pathways is $20.1 per tonne-$CO_2e$, primarily due to higher carbon capture efficiency and effective heat integration. Blue ammonia routes thus tend to be more economically attractive in countries with low-cost, stable natural gas resources, whereas regions with expensive gas or high financing costs exhibit notably higher blue ammonia production costs. On average, the Middle East demonstrated the lowest blue ammonia costs ($0.49 per kg$NH_3$), while

Europe, benefiting from relatively decarbonized electricity grids and more efficient gas infrastructure, showed the lowest WTG emissions (about 0.56 $kgCO_2e$ per $kgNH_3$).

By contrast, electrolytic ammonia (PEMEC based LTE, SOEC based HTE) driven solely by grid power usually showed both more expensive and more carbon-intensive than gray ammonia in many regions, underscoring the importance of low-carbon grid electricity sources. Nevertheless, in countries with cheaper electricity or predominantly low-carbon grids, the economic and environmental advantage of electrolytic ammonia becomes clearer. Moreover, in most regions, the levelized cost of dedicated renewable power was already lower than typical industrial grid prices. Although variable renewables could lower the effective capacity factor or raise costs of additional storage (battery or hydrogen buffer), this study finds that many regions can already produce green ammonia at a lower cost than grid-based (yellow) ammonia. China emerges as having the lowest green ammonia costs (\$0.55 per $kgNH_3$), primarily due to its low renewable electricity cost.

Global trade results show that maritime transportation and port storage can add \$0.07–\$0.20 per $kgNH_3$ to the total supply chain cost and 0.02–0.18 $kgCO_2e$ per $kgNH_3$ in GHG emissions, scaling with the voyage distance. Exporters in regions with highly favorable production economics—whether due to cheap natural gas or low-cost renewables—can often supply ammonia at lower overall cost to high-cost regions than those regions can achieve through domestic production, even after accounting for transport expenses. In terms of GHG emissions, upstream differences in natural gas extraction and processing dominate in blue ammonia routes; thus, low-upstream-emission exporters such as Norway, some Northern Europe or Middle Eastern countries achieved superior well-to-port carbon footprints. For green ammonia, transport-related emissions become relatively more significant (since production is nearly carbon-free), favoring shorter-distance trade or intra-regional sourcing. We also note that if production costs and emissions exceed certain thresholds, using ammonia cargo as shipping fuel may become less economically or environmentally beneficial due to the added amplification effect of producing more ammonia to cover ship fuel usage.

Furthermore, the sensitivity analysis confirms how strongly ammonia supply chain costs and emissions depend on natural gas prices, electricity price, WACC, CAPEX, capacity factor, and renewable energy integration scenarios (reduced capacity factor operation, ESS implementation, hydrogen tank utilization). Where gas prices remain the main driver for gray/blue ammonia, the cost and carbon intensity of electricity, plus capacity factors, dominate electrolytic ammonia routes. VRE integration scenarios present both challenges and opportunities, with hydrogen storage scenarios offering the greatest economic advantages in most regions.

Finally, future pathway analysis utilizing this study's database quantitatively presents the achievable cost-environmental performance and clear trade-off frontier in decarbonizing the ammonia supply chain. Fully shifting to blue ammonia enables a 70.9% GHG emission reduction with a 23.2% increase in total supply chain costs, while shifting to green ammonia enables a 99.7% GHG reduction with a 46.0% total cost increase. These low-carbon production pathways are projected to operate with CO_2e avoidance costs ranging from \$68 to 97 per tonneCO_2e across the supply chain. During shipping, use of NH_3 boil-off is advantageous for both economics and emissions, whereas using cargo-ammonia as fuel is a conditional strategy that should depend on depending on whether the production method is low-carbon and its resulting unit price.

Overall, this study presents the largest and most unified framework for evaluating the economic and environmental implications of ammonia as an expanding energy carrier beyond its traditional fertilizer and industrial role. This integrated study overcomes previous limitations caused by fragmented international ammonia supply chain data derived from diverse case studies and their inconsistent methodologies. The resulting global dataset can support supply chain optimization modelling, informed decision-making in technology selection, investment prioritization, and policy development, especially as ammonia's relevance in sustainable energy systems continues to grow. Building on this framework, future research can explore more extensive modeling of ammonia end-use applications, integrate cross-border carbon regulations or incentives, and pursue global-scale optimization of low-carbon ammonia supply chains.

Author contributions

Woojae Shin: writing – original draft, investigation, formal analysis, database building, writing – review and editing; Haoxiang Lai: investigation, resources; Gasim Ibrahim: investigation, validation; Guiyan Zang: conceptualization, writing – review and editing, supervision.

Conflicts of interest

The authors have no competing financial interests or personal relationships that could have appeared to influence the work reported in this paper.

Data availability

The data supporting this article have been included as part of the supplementary information and supplementary data (SI). Supplementary information: detailed methodologies, background data for analysis, and detailed results value. See DOI: https://doi.org/10.1039/d5ee05571g.

Acknowledgements

The authors would like to thank the financial support from the MIT Energy Initiative (MITEI) Future Energy Systems Center for the project ''Supply Chain Analysis of Ammonia as Hydrogen Carrier''.

References

1 IEA, *Ammonia Technology Roadmap: Towards More Sustainable Nitrogen Fertiliser Production*, Report 9264965688, OECD Publishing, 2021.
2 J. R. A. Peter Aagaard, T. Nauclér, P. Prabhala and K. Wedege, *From green ammonia to lower-carbon foods*, https://www.mckinsey.com/industries/agriculture/our-insights/from-green-ammonia-to-lower-carbon-foods).
3 F. Bird, A. Clarke, P. Davies and E. Surkovic, *The Royal Society*, Policy Briefing, London, UK, 2020.
4 G. Wang, J. Zhao, H. Zhang, X. Wang, H. Qin, K. Wu, C. Zhao, W. Fan and J. Xu, *Energy Fuels*, 2024, **38**, 15861–15886.
5 H. M. Almajed, O. J. Guerra-Fernández and D. Rough, *Analysis of Hydrogen Supply Chain Readiness in Selected Indo-Pacific Countries*, National Renewable Energy Lab.(NREL), Golden, CO (United States), 2025.
6 IRENA, *Global Hydrogen Trade to Meet the 1.5 °C Climate Goal – Part 1; Trade Outlook for 2050 and Way Forward*, International Renewable Energy Agency Abu Dhabi, United Arab Emirates, 2022.
7 IRENA, *Global Hydrogen Trade to Meet the 1.5 °C Climate Goal – Part 2; Technology Review of Hydrogen Carriers*, International Renewable Energy Agency Abu Dhabi, United Arab Emirates, 2022.
8 IRENA and Ammonia Energy Association, *Innovation Outlook: Renewable Ammonia*, 2022.
9 H. Brinks, O. Ivashenko, B. Bakken, T. Wang and H. Tvete, *DNV White Paper*, 2024.
10 S. Mingolla and L. Rosa, *Nat. Food*, 2025, 1–12.
11 G. Gaulier and S. Zignago, *CEPII Working Paper 2010-23*, 2023, Available at SSRN: https://ssrn.com/abstract=1994500 or , DOI: 10.2139/ssrn.1994500.
12 H. Ishaq and C. Crawford, *Energy Convers. Manage.*, 2024, **300**, 117869.
13 T. Terlouw, L. Rosa, C. Bauer and R. McKenna, *Nat. Commun.*, 2024, **15**, 7043.
14 D. Tonelli, L. Rosa, P. Gabrielli, K. Caldeira, A. Parente and F. Contino, *Nat. Commun.*, 2023, **14**, 5532.
15 L. Rosa and P. Gabrielli, *Environ. Res. Lett.*, 2022, **18**, 014008.
16 A. Oni, K. Anaya, T. Giwa, G. Di Lullo and A. Kumar, *Energy Convers. Manage.*, 2022, **254**, 115245.
17 IEA, *Energy Technology Perspectives 2024*, 2024.
18 Clean Air Task Force, *Hydrogen for decarbonization: a realistic assessment*, 2023.
19 S. Giddey, S. Badwal, C. Munnings and M. Dolan, *ACS Sustainable Chem. Eng.*, 2017, **5**, 10231–10239.
20 L. Zhai, S. Liu and Z. Xiang, *Ind. Chem. Mater.*, 2023, **1**, 332–342.
21 D. Tonelli, L. Rosa, P. Gabrielli, A. Parente and F. Contino, *Nat. Food*, 2024, **5**, 469–479.
22 S. C. D'Angelo, A. J. Martín, S. Cobo, D. F. Ordóñez, G. Guillén-Gosálbez and J. Pérez-Ramírez, *Energy Environ. Sci.*, 2023, **16**, 3314–3330.
23 S. Santos, G. Collodi, G. Azzaro and N. Ferrari, *IEAGHG*, 2017.
24 A. Laval, H. T. Hafnia and S. G. Vestas, *Hafnia*, 2020, **7**, 32–59.
25 K. Lee, X. Liu, P. Vyawahare, P. Sun, A. Elgowainy and M. Wang, *Green Chem.*, 2022, **24**, 4830–4844.
26 X. Liu, A. Elgowainy and M. Wang, *Green Chem.*, 2020, **22**, 5751–5761.
27 E. R. Morgan, J. F. Manwell and J. G. McGowan, *ACS Sustainable Chem. Eng.*, 2017, **5**, 9554–9567.
28 P. Mayer, A. Ramirez, G. Pezzella, B. Winter, S. M. Sarathy, J. Gascon and A. Bardow, *iScience*, 2023, **26**(8), 107389.
29 R. Nayak-Luke, R. Bañares-Alcántara and I. Wilkinson, *Ind. Eng. Chem. Res.*, 2018, **57**, 14607–14616.
30 S. A. Nosherwani and R. C. Neto, *J. Energy Storage*, 2021, **34**, 102201.
31 L. Pan, J. Li, J. Huang, Q. An, J. Lin, A. Mujeeb, Y. Xu, G. Li, M. Zhou and J. Wang, *iScience*, 2023, **26**(12), 108512.
32 C. A. Del Pozo and S. Cloete, *Energy Convers. Manage.*, 2022, **255**, 115312.
33 M. Rivarolo, G. Riveros-Godoy, L. Magistri and A. F. Massardo, *ChemEngineering*, 2019, **3**, 87.
34 M. Tjahjono, I. Stevani, G. A. Siswanto, A. Adhitya and I. Halim, *Int. J. Renewable Energy Dev.*, 2023, **12**(6), 1030–1040.
35 S. Vinardell, P. Nicolas, A. M. Sastre, J. L. Cortina and C. Valderrama, *ACS Sustainable Chem. Eng.*, 2023, **11**, 15975–15983.
36 A. Kakavand, S. Sayadi, G. Tsatsaronis and A. Behbahaninia, *Int. J. Hydrogen Energy*, 2023, **48**, 14170–14191.
37 J. Boyce, R. Sacchi, E. Goetheer and B. Steubing, *Heliyon*, 2024, **10**(6), e27547.
38 R. M. Nayak-Luke and R. Bañares-Alcántara, *Energy Environ. Sci.*, 2020, **13**, 2957–2966.
39 Y. Bicer and I. Dincer, *J. Cleaner Prod.*, 2018, **170**, 1594–1601.
40 D. T. Dong, A. Schönborn, A. Christodoulou, A. I. Ölcer and J. González-Celis, *Proc. Inst. Mech. Eng., Part M*, 2024, **238**, 531–542.
41 C. F. Guerra, L. Reyes-Bozo, E. Vyhmeister, M. J. Caparrós, J. L. Salazar and C. Clemente-Jul, *Renewable Energy*, 2020, **157**, 404–414.
42 J. Huang, H. Fan, X. Xu and Z. Liu, *J. Mar. Sci. Eng.*, 2022, **10**, 1969.
43 B. Bonnet-Cantalloube, M. Espitalier-Noël, P. F. de Carvalho, J. Fonseca and G. Pawelec, *Hydrogen Europe*, 2023.
44 ISPT, *Power to Ammonia*, ISPT, 2017.
45 T. Kroon, A. Fattahi, F. Dalla Longa, C. Slootweg and B. Van der Zwaan, *Sustainable Energy Fuels*, 2025, **9**, 1773–1785.
46 O. Schuller, J. Bopp and J. Rapp, *1st Life Cycle GHG Emission Study on the Use of Ammonia as Marine Fuel-produced for SGMF*, Sphera Solutions, 2024.
47 W. J. Shin, Y. Lee, Y. Yu, M. Ko, C. Lee and H. H. Song, *J. Cleaner Prod.*, 2023, 138907.
48 H. Lai, L. Deng, A. Menon, E. Gençer, A. Ghoniem, R. J. Stoner and G. Zang, *Energy Conversion and Management*, 2026.
49 IEA, *Global hydrogen review 2023*, International Energy Agency, Paris, 2023.
50 IEA, *The Future of Hydrogen*, OECD Publishing, Paris, 2019.

51 G. Ibrahim, B. Lin, J. Garrido, W. Shin, H. Lai, A. M. Bala, B. Gebreslassie, L. Nagendran, D. Heston, T. W. Wu and G. Zang, *Fuel*, 2026.
52 B. Mirletz, L. Vimmerstedt, G. Avery, A. Sekar, D. Stright, D. Akindipe, S. Cohen, W. Cole, P. Duffy and A. Eberle, *Annual Technology Baseline: The 2024 Electricity Update*, National Renewable Energy Laboratory (NREL), Golden, CO (United States), 2024.
53 G. Zang, E. J. Graham and D. Mallapragada, *Int. J. Hydrogen Energy*, 2024, **49**, 1288–1303.
54 W. Shin, B. Lin, H. Lai, G. Ibrahim and G. Zang, *Green Chem.*, 2025, **27**, 3655–3675.
55 A. Santecchia, R. Castro-Amoedo, T.-V. Nguyen, I. Kantor, P. Stadler and F. Maréchal, *Energy Environ. Sci.*, 2023, **16**, 5350–5370.
56 Ammonia Energy Association, Fit for 55: Tax breaks, border tariffs, and Guarantees of Origin in the EU).
57 IEA, *Projected Costs of Generating Electricity*, 2020.
58 D. Ayres and L. Zamora, *IRENA: Masdar City*, United Arab Emirates, 2024, p. 211.
59 Compass International Inc, *Location factors database*, 2017.
60 A. Damodaran, *Measures and Implications-The*, 2022.
61 M. Wang, A. Elgowainy, U. Lee, K. H. Baek, A. Bafana, P. T. Benavides, A. Burnham, H. Cai, V. Cappello, P. Chen, Y. Gan, U. R. Gracida-Alvarez, T. R. Hawkins, R. K. Iyer, J. C. Kelly, T. Kim, S. Kumar, H. Kwon, K. Lee, X. Liu, Z. Lu, F. Masum, C. Ng, L. Ou, K. Reddi, N. Siddique, P. Sun, P. Vyawahare, H. Xu and G. Zaimes, 2022, GREET **2022**, DOI: 10.11578/GREET-Excel-12022/dc.20220908.20220901.
62 IEA, *Towards hydrogen definitions based on their emissions intensity*, OECD Publishing, 2023.
63 U.S., IRA, Section 45V Credit for Production of Clean Hydrogen; Section 48(a)(15) Election To Treat Clean Hydrogen Production Facilities as Energy Property, 2023.
64 Energy Newspaper, ''No more than 4 kilograms of CO2 per kilogram of hydrogen''...a clean hydrogen certification standard (in Korean), https://www.energy-news.co.kr/news/articleView.html?idxno=87343, (accessed 14 August, 2023).
65 V. Masson-Delmotte, P. Zhai, A. Pirani, S. L. Connors, C. Péan, S. Berger, N. Caud, Y. Chen, L. Goldfarb and M. Gomis, *Climate Change 2021: The Physical Science Basis.* Contribution of Working Group I to the Sixth Assessment Report of the Intergovernmental Panel on Climate Change, IPCC, Cambridge, United Kingdom and New York, NY, USA, 2021.
66 H.-O. Pörtner, D. C. Roberts, M. Tignor, E. S. Poloczanska, K. M. A. Alegría, M. Craig, S. Langsdorf, S. Löschke, V. Möller, A. Okem and B. Rama (eds.), *Climate Change 2022: Impacts, Adaptation, and Vulnerability. Contribution of Working Group II to the Sixth Assessment Report of the Intergovernmental Panel on Climate Change*, IPCC, Cambridge, UK and New York, NY, USA, 2022.
67 P. R. Shukla, J. Skea, R. Slade, A. Al Khourdajie, R. Van Diemen, D. McCollum, M. Pathak, S. Some, P. Vyas and R. Fradera, *Climate Change 2022: Mitigation of Climate Change.* Contribution of Working Group III to the Sixth Assessment Report of the Intergovernmental Panel on Climate Change, IPCC, Cambridge, UK and New York, NY, USA, 2022.
68 IEA, *Emissions Factors 2023*, Paris, 2023.
69 Carbonfootprint, *Country Specific Electricity Grid Greenhouse Gas Emission Factors – 2023*, 2023.
70 UK Department for Energy Security & Net Zero, *International industrial energy prices*, 2025.
71 D. Peterson, J. Vickers and D. DeSantis, *DOE hydrogen fuel cells program record*, 2020, **19009**.
72 E. Gençer, S. Torkamani, I. Miller, T. W. Wu and F. O'Sullivan, *Appl. Energy*, 2020, **277**, 115550.
73 G. Bilicic and S. Scroggins, *Lazard's Levelized Cost of Energy Analysis—Version 16.0*, 2023.
74 Food and Agriculture Organization of the United Nations, FAOSTAT, https://www.fao.org/faostat/en/#data/RFN, (accessed Oct 28, 2025).

